

NATIONAL ADVISORY COMMITTEE FOR AERONAUTICS

WARTIME REPORT

ORIGINALLY ISSUED
February 1945 as
Memorandum Report L5B23

TESTS OF A $\frac{1}{14}$ -SCALE POWERED MODEL OF THE XB-36

AIRPLANE IN THE LANGLEY 19-FOOT PRESSURE TUNNEL

I - STALLING CHARACTERISTICS AND AILERON EFFECTIVENESS

OF SEVERAL WING AND FLAP ARRANGEMENTS

By S. R. Alexander and James C. Sivells

Langley Memorial Aeronautical Laboratory
Langley Field, Va.

NACA

WASHINGTON

NACA WARTIME REPORTS are reprints of papers originally issued to provide rapid distribution of advance research results to an authorized group requiring them for the war effort. They were previously held under a security status but are now unclassified. Some of these reports were not technically edited. All have been reproduced without change in order to expedite general distribution.

MR No.- 15B23

NATIONAL ADVISORY COMMITTEE FOR AERONAUTICS

MEMORANDUM REPORT

for the

Army Air Forces, Air Technical Service Command

TESTS OF A $\frac{1}{14}$ -SCALE POWERED MODEL OF THE XB-36

AIRPLANE IN THE LANGLEY 19-FOOT PRESSURE TUNNEL

I - STALLING CHARACTERISTICS AND AILERON EFFECTIVENESS

OF SEVERAL WING AND FLAP ARRANGEMENTS

By S. R. Alexander and James C. Sivells

SUMMARY

An investigation was conducted in the Langley 19-foot pressure tunnel to determine the stalling characteristics, aileron effectiveness, and, to a limited extent, the longitudinal stability of a $\frac{1}{14}$ -scale model of the XB-36 airplane.

The model was tested with the original wing-flap configuration and with several modifications to the outboard panels and flap arrangement. The modifications to the outboard wing panels consisted of (1) the original panels with mid-chord slots ahead of the ailerons, and (2) a revised panel which incorporated changes in airfoil section, twist, plan form, and aileron area. The flap arrangements included full- and partial-span, single- and double-slotted configurations.

With the original wing and the full-span flap arrangement the model exhibited unsatisfactory stalling characteristics, insufficient aileron effectiveness, particularly with flaps deflected, and longitudinal instability after the stall with flaps deflected. The slotted panels were better than the revised panels in improving the stalling characteristics. None of the configurations tested, however, produced satisfactory stalling characteristics. The configuration with the revised panels exhibited better aileron effectiveness, which is attributed mainly to the increase in aileron area. With flaps deflected, the greatest improvement in aileron effectiveness was realized by changing the flap configuration from full span to

partial span. The use of partial-span, double-slotted flaps produced a greater maximum lift coefficient than that obtained with the other flap configurations but caused a large change in trim lift coefficient. The static longitudinal instability after the stall experienced by the model with flaps deflected for take-off and landing was less severe with the modified outboard panels than with the original wing.

INTRODUCTION

The Consolidated Vultee XB-36 airplane is a proposed six-engine, pusher-type, long-range bomber. Tests were conducted on a $\frac{1}{14}$ -scale model in the Langley 19-foot pressure tunnel to determine the stability and control characteristics of the airplane. In the course of this investigation, it was found that the stalling characteristics of the model, in its original configuration, were unsatisfactory. Besides causing a loss in aileron effectiveness near maximum lift, the stall was also accompanied by longitudinal instability after maximum lift was reached, when the flaps were deflected for take-off or landing. Attempts to rectify these unsatisfactory conditions by the use of midchord or leading-edge spoiler arrangements proved inadequate. It was therefore considered inadvisable to continue with the remainder of the testing schedule until some practical solution to this problem was secured.

In a further attempt to improve the stalling characteristics of the airplane, and thereby improve the aileron effectiveness and longitudinal stability at high lift coefficients, it was decided to investigate proposed modifications to the wing and flap arrangement. The manufacturer proposed to incorporate midchord slots in the wing ahead of the ailerons. This proposal would entail a minimum change to the airplane design. The Langley laboratory proposed to eliminate the outboard flaps, to change the inboard flaps from single-slotted to double-slotted flaps, and to revise the outboard wing panels by changing the airfoil section, twist, plan form, and aileron area. Although it was realized that the greatest improvement could be obtained if the entire wing was revised, the revisions proposed by the Langley laboratory were restricted to the outboard wing panels (from 62 percent of the semi-span to the wing tip) to facilitate changes to the airplane

design. These revisions were based upon the theoretical analysis given in the appendix.

Subsequent investigation revealed that, although both proposals produced some improvement, the slotted-panel configuration could be materially improved through elimination of the outboard flaps. Accordingly, this configuration was further investigated with both single- and double-slotted inboard flaps, and, in order to provide comparative data, the NACA panel configuration was also tested with partial-span, single-slotted flaps.

This paper presents the results of stalling, aileron, and some longitudinal stability tests of the original and both modified wing panels, various flap and spoiler arrangements, and full and modified flap-nacelle seals.

COEFFICIENTS AND SYMBOLS

The coefficients and symbols used herein are defined as follows:

C_L lift coefficient, L/qS

C_D drag coefficient, D/qS

C_m pitching-moment coefficient, M/qSc

C_l rolling-moment coefficient, L'/qSb

C_{l_p} rate of change of rolling-moment coefficient with
helix angle, $\frac{\partial C_l}{\partial \frac{pb}{2v}}$

T_c thrust coefficient, $T/\rho v^2 D^2$

L lift, pounds

D drag, pounds; diameter of propeller, feet

M pitching moment, foot-pounds

L' rolling moment, foot-pounds

T effective thrust, pounds

- q dynamic pressure of free stream, $\frac{1}{2}\rho V^2$, pounds per square foot
- S wing area, square feet
- c mean aerodynamic chord (M.A.C.), feet
- b wing span, feet
- $pb/2V$ helix angle, radians
- p rolling velocity, radians per second
- V airspeed, feet per second
- V_i indicated airspeed, miles per hour
- V_s indicated airspeed at maximum lift coefficient, miles per hour
- ρ mass density of air, slugs per cubic foot
- α angle of attack of root chord, degrees
- δ_{f_1} partial-span, single-slotted inboard-flap deflection, degrees
- δ_{f_0} partial-span, balanced-split outboard-flap deflection, degrees
- δ_{f_s} partial-span, double-slotted inboard-flap deflection, degrees
- δ_a left aileron deflection, positive with trailing edge down, degrees
- δ_e elevator deflection, positive with trailing edge down, degrees
- R test Reynolds number, $\rho V c / \mu$
- M Mach number, V/V_c
- μ coefficient of viscosity, pound seconds per square foot
- V_c speed of sound in air, feet per second

- c_l section lift coefficient
- y spanwise location, percent of semispan
- W_1 original wing
- W_2 wing with slotted outboard panels
- W_3 wing with NACA revised outboard panels

MODEL AND TESTS

Model.— The model (fig. 1), with the exception of the wooden empennage and NACA outboard wing panels, was basically of all metal construction. Block inserts containing the slots (figs. 2 and 3) were incorporated in the outboard panels for the W_2 configuration. This outboard panel was replaced by the wooden NACA panel for the tests of W_3 . The model was kept smooth by filling surface irregularities with crack filler and glazing putty and, in addition, the wing was sprayed with lacquer and rubbed in a chordwise direction with number 400 carborundum paper to provide an aerodynamically smooth surface.

Protuberances on the fuselage included sighting blisters, antennae for radio-electronic devices, and air-speed pitot-static masts.

A comparison of the physical characteristics of the wing configurations investigated is given in table I and figures 4 and 5. It should be noted that the additional washout for wing W_3 was obtained by twisting the wing sections about the aileron hinge line.

All the flaps (figs. 5 and 6) were set manually by the use of brackets constructed to give the desired flap deflection. Only the left ailerons, which were of constant chord (figs. 5 and 7), were deflected for the aileron tests. These ailerons were locked manually at the desired deflection and sealed by placing cellulose tape along the gap on both the upper and lower surfaces.

The wing nacelles were constructed with air passages to allow for internal air flow. Duct orifice plates and

plugs at the exits provided means for adjusting the air flow. Total and static pressure tubes were suitably located in the left inboard and outboard nacelles for the measurement of air-flow quantities.

It should be noted that two horizontal tail planes were installed on the model in the course of the investigation. The original tail, which had an area of 4.95 square feet and an aspect ratio of 4.49, was used during most of the stalling and force tests of the original model. The revised tail, which had an area of 4.99 square feet and an aspect ratio of 5.50, was used for the remainder of the tests. The stabilizer was set at -7° to the wing-root chord.

Tests.— The tests were conducted in the Langley 19-foot pressure tunnel with the air in the tunnel compressed to an absolute pressure of about 35 pounds per square inch. The model was mounted on the normal three-support system (fig. 8) and the aerodynamic forces and moments were measured by means of a six-component, simultaneously recording balance system.

With the exception of several stall investigations made with the model propellers in operation, and force tests to determine the effect of the spoilers, the tests presented herein were conducted at a dynamic pressure of approximately 100 pounds per square foot, with the model propellers removed. This value of dynamic pressure corresponds to a Reynolds number of about 4,500,000 and a Mach number of about 0.17.

Wing W_1 was tested at a Reynolds number of about 2,500,000 with operating propellers. The power conditions for full-scale operation were simulated in the wind tunnel by matching the propeller thrust coefficient of the model with that of the airplane at a given lift coefficient. The blade angle was 21° at the 0.75 radius station for all power-on tests. These power ratings were based on sea-level conditions and on a maximum gross weight of 340,000 pounds.

The nacelle openings were adjusted to give average values of entrance velocity ratio and flow coefficient of 0.80 and 0.078, respectively. These values were selected to simulate the nacelle air flow for the full-scale airplane when cruising at 30,000 feet. The first tests made

with the partial-span, double-slotted flaps deflected 50° for landing resulted in a maximum lift coefficient of 1.71. Comparison with the other model configurations tested made it apparent that this flap configuration was not an optimum one. Tests made with the flaps deflected 55° resulted in lower maximum lift coefficients. Therefore, changes in flap gap, vane position, and flap position appeared to be necessary. Because of the model construction, it was not feasible to change the flap or vane position. Consequently, in order to decrease the flap gap, the flap-well lip was extended 0.94 inch along the wing upper surface as shown in figure 6. Tests of this arrangement showed satisfactory increases in maximum lift at the landing-flap deflections. The 50° flap deflection produced a slightly higher maximum lift at a higher angle of attack than the 55° flap deflection. Hence, the 50° flap deflection, with the flap-well lip extended, was used for all tests presented herein in which the double-slotted flaps were deflected for landing.

The basic model configurations tested are given in table II.

RESULTS AND DISCUSSION

The results are presented in the form of standard nondimensional coefficients. The tare and interference effects of the model-support struts were not obtained for all the configurations, and therefore no corrections for these effects were applied to the lift, drag, and pitching-moment coefficients. Jet-boundary and air-flow misalignment corrections were applied to the angle of attack and the drag coefficient. The rolling-moment coefficients due to deflection of the left aileron were corrected for jet-boundary interference and model and tunnel asymmetry.

All coefficients were based on the mean aerodynamic chord and wing area of the actual wings. All moments were measured about the quarter-chord point of the mean aerodynamic chord of wing W_1 so that the slopes of the pitching-moment curves would not change for otherwise similar model configurations.

In the course of the investigation, the original tail plane was replaced by the revised tail plane. The test results presented are for the revised tail except where

otherwise noted. A list of the figures presented herein is given in table III and the results obtained from the force tests are summarized in table IV. Included in table IV are values for W_3 based on the wing area of W_1 to facilitate comparison at the same airspeed and airplane weight. Values of drag coefficient are given for a lift coefficient of 0.4 (high-speed condition) and 0.8 (cruising condition).

Stalling Characteristics

The stalling characteristics of the several model configurations were determined by the observation of tufts attached to the upper surface of the wing at the 30-, 50-, 70-, and 90-percent wing-chord stations and spaced about 5 inches spanwise. At every angle of attack at which the flow pattern changed, sketches and moving-picture records were obtained. All values of lift coefficient presented on the stall diagrams were obtained with the tufts in place. The value of the data insofar as the determination of the stalling characteristics of the wing are concerned will not be affected by the tail configuration tested.

Wing W_1 . - The stalling characteristics observed for this model configuration with flaps retracted and with flaps deflected for landing are shown in figure 9. At the Reynolds number of about 2,500,000 the model propellers were operated to give zero thrust throughout the lift range investigated. At the Reynolds number of 5,500,000, the propellers were removed.

In general, the stall started at the trailing edge of the wing adjacent to the outboard nacelles and progressed outboard and forward. The inboard sections partially stalled, in most cases, after the outboard panels were completely stalled. The rate of stall progression over the outer wing panels appeared to be more rapid when the flaps were deflected. These results indicated unsatisfactory stall progression which, as will be shown later, was accompanied by a loss of aileron effectiveness near maximum lift coefficient, and longitudinal instability after maximum lift coefficient was reached. The nature of this stall is such that the pilot may lose control of the airplane before being adequately warned. The actual stalling characteristics for flap neutral are in fair agreement with those predicted by an analysis of the spanwise section-lift-coefficient distribution (see appendix).

The analysis indicates that the stall at the full-scale Reynolds number would be more severe than that shown by the model tests.

Upon the suggestion of the manufacturer, three spoilers of different vertical heights were tested on the model in an attempt to induce initial stall over the inboard panel at high values of lift coefficient. These spoilers were located on the 40-percent chord line of the wing upper surface and extended from the fuselage to the center line of the center nacelles. The vertical heights of the spoilers were approximately 0.22, 1.0, and 2.0 percent of the wing-root chord, c_R . The 0.22-percent c_R spoiler did not affect the original stall pattern. The 1.0- and 2.0-percent c_R spoilers caused a complete stall behind the spoiler throughout the lift range investigated. It was therefore concluded that, for this model, these spoiler arrangements were unsatisfactory.

In a further attempt to produce better stalling characteristics for the model, tests of a leading-edge spoiler arrangement were included in the investigation. The sharp-nose, leading-edge spoiler was located on the model as shown in figure 10. It was estimated that, for this position, the stagnation point would occur at the sharp edge at zero lift. A similar arrangement with the sharp edge located in such a manner as to coincide with the stagnation point for $C_L = 0.8$ was found to have little effect on the stall progression. In an effort to minimize the effect of the spoiler on the drag of the model, the sharp leading edge was made to include an angle of 90° with sides faired to the wing-section profile.

Diagrams of the stall progression with and without the spoilers and at comparable model configurations are presented in figure 11 for two power conditions. The leading-edge spoiler arrangement did not change the stall pattern at low lift coefficients, but produced intermittent stall at the root sections at higher lift coefficients. A comparison of the spoiler-off data of figure 11 with the data of figure 9(a) indicates that increasing the thrust coefficient tends to clean up the stalled area at the root.

The results of force tests made on the model with propellers removed and with and without the leading-edge

spoiler are presented in figure 12. The spoiler decreased the maximum lift coefficient 0.12 and 0.04 for the normal and landing conditions, respectively, but increased the drag coefficient about 0.0020 below a lift coefficient of 0.8 for the normal condition. The static longitudinal instability, after maximum lift coefficient, indicated by the pitching-moment curve of the model, was not as severe with the spoilers on as with the spoilers off.

This spoiler arrangement was not considered an acceptable solution to the unsatisfactory stall of the model inasmuch as the stall progression was not improved. In addition, the increase in drag, with flaps retracted, at moderate lift coefficients and the loss in maximum lift coefficient with flaps retracted and deflected were deemed prohibitive.

Wing W₂, with full-span flaps.- The stall progression for this model configuration is presented in figure 13(a). The stall started at approximately the same place as on the original wing and gradually progressed inboard. The midchord slots apparently retarded the stall progression outboard of the outboard nacelles although the flow over the ailerons through most of the lift range was very rough.

Wing W₂, with partial-span, single-slotted flaps.- The stall studies made with this model configuration with flaps deflected for take-off and landing are presented in figure 13(b). In general, the stall progression was similar for both flap conditions. The rough flow over the ailerons typical of the slotted panels was not affected by the change in flap configuration.

Wing W₂, with partial-span, double-slotted flaps.- The stall studies for this model configuration are shown in figure 13(c). The flap neutral characteristics are reproduced from figure 13(a). This configuration with flaps deflected for landing may be worse than the other flap configurations inasmuch as the stall over the flaps was decreased, thereby decreasing the chances for a stall warning for the pilot. On the other hand, the stalled aileron area at maximum lift was slightly decreased. The regions of rough flow over the ailerons were not affected by the change in flap configuration.

Wing W₃. - The stalling characteristics of the NACA arrangement are shown in figure 14. These panels showed some improvement over the original panels for the flap-neutral condition inasmuch as the center sections stalled before the ailerons completely stalled. The stall over the ailerons was not delayed as much with these panels as with the slotted panels. With flaps deflected, the stall over the ailerons was but slightly delayed by these panels as compared with the original wing and the stall over the flaps was eliminated by the action of the double-slotted flaps.

The improvement in the flap-neutral stalling characteristics predicted from the analysis presented in the appendix was only partially realized in the actual case possibly because of the break in the wing leading edge resulting from sweeping forward the leading edge of the outboard panels. As in the case of wing W₁, the analysis indicates that the stall at the full-scale Reynolds number would be more severe than that shown by the model tests.

Aileron Characteristics

The lift and rolling-moment characteristics of the model with the left aileron deflected were determined from tests made at a Reynolds number of about 4,500,000 with the model propellers removed. The results of these tests were used to estimate the aileron rolling effectiveness of the airplane in terms of the developed helix angle, $pb/2V$. This helix angle is estimated to be approximately equal to $\frac{0.8C_l}{C_{lp}}$, where C_{lp} is dependent upon the aspect and taper ratios of the wing plan form. The values of C_{lp} for both wing plan forms were calculated from lifting-line theory to which an edge-velocity correction was applied (method similar to that used in reference 1). These values were determined to be 0.548 for W₁ and W₂ and 0.563 for W₃. The indicated airspeed was computed for the normal gross weight of 265,000 pounds, using the untrimmed lift coefficient obtained with zero elevator deflection.

Wing W₁. - The aileron characteristics for the original wing with the left aileron deflected over the range, -20° to 20° , are presented in figure 15. The aileron rolling

effectiveness, calculated in terms of the estimated helix angle $pb/2V$ for the airplane in the normal and landing configuration is shown in figure 16. The requirement for satisfactory aileron effectiveness, $pb/2V = 0.07$ at 110 percent of the stalling speed, prescribed in reference 2, will probably not be met by the airplane for any of the flap configurations tested. A value of $pb/2V$ of 0.07 was obtained at higher speeds with the model equipped with the partial-span, single-slotted flaps deflected for landing. It can clearly be seen that the outboard flaps were detrimental to the aileron effectiveness, particularly when the aileron was deflected down. Near the stall, the rolling moment due to the down aileron became negative. This loss in effectiveness results from the close proximity of the down aileron and the deflected flap as shown in figure 6(b). A value of $pb/2V$ of only 0.031 was obtained at 110 percent of the stalling speed with the full-span flaps deflected, while a value of 0.052 was obtained with the partial-span flaps only. Both of these values were low as a result of the tip stall experienced with this wing.

Wing W_2 . - The aileron characteristics for the model with the slotted panels are presented in figure 17. These results are presented for flaps neutral and for the three types of flaps deflected for landing. The left aileron was deflected over the range -25° to 20° for the condition with the partial-span, double-slotted flaps and -20° to 20° for the flaps neutral, the full-span and the partial-span, single-slotted flaps. The estimated helix angle for these flap conditions are presented in figure 18. The addition of the midchord slots did not appreciably increase the aileron effectiveness at 110 percent of the stalling speed even though they did produce an improvement in the stalling characteristics. The main effect of the slots was to maintain the rolling effectiveness to lower speeds by increasing the maximum lift coefficient. The slots, however, caused loss of aileron rolling effectiveness throughout most of the climbing to high-speed range and, with flaps deflected, caused complete loss of effectiveness near the stalling speed. A large improvement in rolling effectiveness was obtained at low speeds by changing the flap configuration from full-span to partial-span, thereby eliminating the interference effects of the outboard flaps on the flow over the ailerons. The rolling moment due to the down aileron, however, still became negative near maximum lift coefficient. An acceptable value of $pb/2V$ of 0.07 was attained at 110 percent of the stalling speed

with differential aileron deflections of -25° and 20° for the condition with partial-span, double-slotted flaps. It should be noted that it will be much more difficult to balance the aileron at the -25° deflection than at the -20° deflection because of the rapid, nonlinear increase in hinge-moment coefficients in this range of aileron deflections. On the other hand, the -25° deflection may not be necessary if the aileron area is increased to provide satisfactory control for the flap-neutral condition.

Wing W_3 .-- Figures 19 and 20 present the aileron characteristics and estimated helix angle, respectively, for the model equipped with the NACA outer panels. With the differential aileron deflection, the satisfactory aileron rolling effectiveness requirements are met at 110 percent of the stalling speed and are exceeded for higher speeds. This configuration, with its increased aileron area, produced the greatest $pb/2V$ value of any of the configurations tested. The aileron effectiveness, furthermore, is maintained beyond the stall, a condition which was not realized for either the W_1 or W_2 configuration. Again, the aileron balance problem at the -25° deflection is quite important, although in this case, this deflection may be decreased a few degrees without decreasing the helix angle below 0.07. A comparison of the values of $pb/2V$ at a given indicated airspeed makes the superior aileron effectiveness of W_3 still more apparent.

Lift, Drag, and Pitching-Moment Characteristics

The lift, drag, and pitching-moment characteristics of the model with the several wing outer panels and flap configurations were determined from tests made at a Reynolds number of approximately 4,500,000. The stabilizer was set at -7° to the wing-root chord and, with two exceptions in which the deflection was -10° (figs. 23(b) and 24(b)), the elevator was set at 0° .

All of these tests were made with the revised horizontal tail plane installed on the model.

Wing W_1 .-- Some tests were made with fixed transition to show the effect of surface roughness on drag and longitudinal stability. The transition was fixed (fig. 21) at 11 percent of the wing chord (approximate location of the front spar on the airplane). The lift, drag, and pitching-

moment characteristics are presented in figure 22. The fixed transition increased the maximum lift coefficient, increased the drag below a lift coefficient of 1.1, and did not affect the pitching moment appreciably. The longitudinal instability at the stall associated with this model-wing configuration with full-span flaps is apparent from an examination of the pitching-moment curves of figure 22. This instability is less severe with the partial-span, single-slotted flaps and is not indicated with flaps retracted.

Wing W₂.-- The lift, drag, and pitching-moment characteristics for this model configuration are presented in figure 23. The addition of the slots increased the maximum lift coefficient for all three flap deflections tested. The longitudinal instability at the stall has been reduced for the take-off and landing configurations. The slots did not appreciably affect the trimmed lift coefficient of the model with elevator neutral.

The characteristics of the model with the partial-span, double-slotted flaps deflected for landing and with the elevator set at 0° and -10° are presented in figure 23(b). This flap configuration produced a still greater maximum lift than was obtained with the other flap configurations. The large change in trim lift coefficient experienced by the model when the double-slotted flaps were deflected, however, would probably cause an undesirable control condition. This situation probably resulted from the increased downwash over the horizontal tail surfaces caused by the high concentration of lift at the wing center section when the double-slotted flaps were deflected.

Wing W₃.-- The results of tests made on the model to determine the aerodynamic characteristics of the NACA panels with partial-span, single- and double-slotted flaps are presented in figure 24. With the partial-span, single-slotted flaps deflected for landing, the NACA panels produced a lower value of maximum lift coefficient than the W₁ and W₂ configurations. The landing speed of W₃ would, however, be the same as W₁ if no change in weight were involved because of the greater wing area of W₃. With flaps neutral and natural transition, the drag characteristics of this wing are essentially similar to that of the original and slotted wing panels. The effect of fixing the transition at 11 percent of the wing chord for the flaps-retracted condition was, in general, similar

to that for fixed transition on the original panels. The maximum lift coefficient obtained with the partial-span, double-slotted flaps deflected for landing was lower for this wing configuration than for the slotted panels.

In an attempt to increase further the maximum lift, full and modified seals between the flaps and nacelles were added as shown in figure 25. The seals showed a loss in maximum lift coefficient rather than an improvement (fig. 26).

Static longitudinal instability after the stall was equally present for the W_3 as for the W_2 configuration, but was not as severe as for the W_1 configuration.

Model Configuration for Further Tests

At the completion of the tests described herein, the manufacturer decided to incorporate, in the design of the first airplane, the configuration with the slotted panels and the partial-span, single-slotted flaps (the slots in the panels are intended to be closed when the flaps are retracted). This decision was made on the basis of the results of the tests and from a consideration of the problems involved in the production of the airplane.

The configuration selected has about the least unsatisfactory stalling progression of any tested. The elimination of the outboard flap materially improved the aileron effectiveness. Some sacrifice in maximum lift coefficient is involved in this selection since an increase in maximum lift coefficient could be realized if the double-slotted flap configuration had been selected.

On the basis of the manufacturer's decision, the configuration selected was used for further tests in the Langley 19-foot pressure tunnel to determine the lateral and longitudinal stability and control characteristics of the model.

CONCLUSIONS

The following conclusions are indicated by tests of a $\frac{1}{11}$ -scale model of the XB-36 airplane with several wing and flap configurations:

1. The stalling progressions of all configurations tested are considered to be unsatisfactory. The stall of the original configuration originates at the outboard nacelles and progresses gradually outboard enveloping the tips before the inboard-section stalls. The slotted panels are more effective than the NACA panels in delaying the stall over the ailerons. This delay allows the stall to move inboard, except for the configuration with the double-slotted flaps deflected where the action of the flaps cleans up the stall over the center sections. Although the slotted panels retard the stall over the ailerons, there remains a considerable amount of rough flow behind the slots.

2. It is estimated that about 86 percent of the required value of $pb/2V$ (0.07) can be obtained at 110 percent of the stalling speed, with the original configuration with flaps neutral. When the full-span flaps are deflected, a serious loss in rolling effectiveness is experienced. The addition of the midchord slots in the outboard panels does not appreciably increase the aileron effectiveness at 110 percent of the stalling speed even though the stall over the outboard panels is delayed. At speeds higher than 110 percent of the stalling speed, the slots lower the aileron effectiveness, except for the condition of full-span flaps deflected. A large increase in effectiveness, at 110 percent of the stalling speed, is realized when the flap configuration is changed from full span to partial span. With differential deflection, -25° and 20° , of the ailerons, it is estimated that a value of $pb/2V$ equal to 0.07 can be obtained with the condition of partial-span, double-slotted flaps deflected and slots open in the outboard panels. With the NACA outboard panels, which have greater aileron area, the required value of $pb/2V$ equal to 0.07 is exceeded with differential aileron deflection, -25° and 20° , for both the conditions of flaps neutral and with partial-span, double-slotted flaps deflected for landing.

3. The greatest maximum lift coefficient is obtained with the configurations incorporating the slotted panels. The partial-span, double-slotted flaps produce a greater increment of maximum lift coefficient than either the full-span or the single-slotted flap arrangement. There is little difference between the maximum lift coefficient obtained with the original panels and that obtained with the NACA panels. The addition of flap-nacelle seals slightly decreases the maximum lift coefficient for W_3 .

4. The longitudinal instability at the stall experienced with flaps deflected on the original wing was not as severe for either the slotted or the NACA panels. The partial-span, double-slotted flaps cause a much greater change in trim than either the full-span or the single-slotted flap configuration.

Langley Memorial Aeronautical Laboratory
National Advisory Committee for Aeronautics
Langley Field, Va., February 23, 1945

APPENDIX

THEORETICAL ANALYSES FOR WINGS, W_1 AND W_3

The analyses for wings W_1 and W_3 were made for only the flap-neutral condition because of the inadequacy of such analyses for flap-deflected conditions. The effects of fuselage, nacelles, ducts, and the sweepback of the wings could not be taken into account in the method used for analysis. It was realized that sweepback might have an adverse effect on the stalling characteristics but any improvement gained by altering the wing design should be apparent whether or not the effect of sweepback is included in the analyses.

The method of analysis is that described in reference 3. This method consists essentially of determining the point at which the curve of the spanwise distribution of the section lift coefficient becomes tangent to the curve of the spanwise variation of the maximum lift coefficient of each section (see figs. 27 and 28). The spanwise location of the point of tangency represents the point at which stalling is expected to begin. The margin between the two curves is an indication of the manner in which the stall will progress. To avoid tip stalling, it is recommended in reference 4 that there should be a margin of at least $c_l = 0.1$ at 0.70 of the semispan. The value of the wing lift coefficient required to make the curves tangent is the theoretical maximum lift coefficient obtainable. The maximum lift coefficient of each section was obtained from section data for the particular Reynolds number and thickness of each section. The section lift coefficient was also obtained from section data by means of the method of computing the span-load distribution described in reference 5. This method uses actual section data instead of assuming straight-line lift curves.

The results of the analysis for wing W_1 is shown in figure 27. For the model Reynolds number of 5,500,000, the curves indicate that the stall would start from about 0.35 to 0.65 of the semispan and, because of the small margin at 0.70 of the semispan, would spread rapidly toward the tip. For the full-scale Reynolds number of 22,000,000 based upon a speed of about 100 miles per hour, the curves

indicate that the stall would start at about 0.90 of the semispan. These analyses indicate that the stalling characteristics of the model as observed in the tunnel would be unsatisfactory even though the stall would start further inboard than on the full-scale airplane due to the difference in Reynolds number. The effects of the jet boundary on the model stalling characteristics were computed and found to be negligible.

The design of wing W_3 was influenced by a number of factors. Although it was realized that the greatest improvement in stalling characteristics would result from a redesign of the entire wing, practical considerations limited the design to the wing panel outboard of a station approximately 62 percent of the semispan. This station is outboard of the outboard nacelle and approximates the line of detachment of the outboard wing panels on both the model and the full-scale airplane. In order to minimize any increase in drag for the new wing panels, the use of fixed slots was not considered, although such use might improve the stalling characteristics. The tip chord was increased by 50 percent to decrease the taper ratio. This increase was distributed on each side of the original plan form in such a manner as to keep the location of the aerodynamic center of the wing the same as that of the original wing. In order to increase the maximum lift coefficient obtainable at the tip and the angle of attack for this lift coefficient, the tip airfoil section was changed from an NACA 63(420)-517 section to an NACA 65(315)-517 section. As a further prevention against tip stalling, the washout was increased to 3° at approximately the 75-percent semispan station (location of outboard end of aileron tab) and 4° at the tip. This increase in washout was obtained by twisting the wing panel about the aileron hinge line.

The results of the analysis for wing W_3 is shown in figure 28. For the model Reynolds number of 4,700,000, the curves indicate that the stall would start from 0.30 to 0.50 of the semispan and would be more satisfactory than that of W_1 since it would not tend to spread to the tip. For the full-scale Reynolds number, the curves indicate that the stall would start about 0.60 of the semispan. Again, the Reynolds number effect makes the stalling characteristics of the model somewhat optimistic compared to those of the full-scale airplane.

The analyses for the two wings (W_1 and W_3) indicate that the stalling characteristics of W_3 will be better than those of W_1 . The stall will probably start further inboard and not spread outboard as fast. Any effect due to sweepback would also favor W_3 since the sweepback of the outboard panel is reduced about $2\frac{10}{2}$. The improvement in stalling characteristics is obtained at an expense of only about $2\frac{1}{2}$ -percent increase in induced drag for a cruising condition of 288 miles per hour at 30,000 feet altitude and a gross weight of 265,000 pounds.

No analysis for wing W_2 could be made because of the lack of two-dimensional data applicable to this wing.

REFERENCES

1. Swanson, Robert S., and Toll, Thomas A.: Estimation of Stick Forces from Wind-Tunnel Aileron Data. NACA ARR No. 3J29, 1943.
2. Anon.: Stability and Control Requirements for Airplanes. AAF Specification No. C-1815, Aug. 31, 1943.
3. Anderson, Raymond F.: Determination of the Characteristics of Tapered Wings. NACA Rep. No. 572, 1936.
4. Soule, H. A., and Anderson, R. F.: Design Charts Relating to the Stalling of Tapered Wings. NACA Rep. No. 703, 1940.
5. Boshar, John: The Determination of Span Load Distribution at High Speeds by Use of High-Speed Wind-Tunnel Section Data. NACA ACR No. 4B22, 1944.

TABLE I
FLAP AND AILERON CHARACTERISTICS

Wing	Surface	Type	Symbol for deflection	Chord, percent wing chord mid-span of surface	Span, percent wing semispan	Figure
W_1, W_2, W_3	Inboard flap	Slotted	δ_{f_1}	25	42	5(a) 5(b) & 6(a)
W_1, W_2	Outboard flap	Balanced split	δ_{f_0}	20	38	5(a) & 6(b)
W_2, W_3	Inboard flap	Double slotted	δ_{f_s}	27	42	6
W_1, W_2	Aileron	Sealed	δ_a	15	38	5(a) & 7
W_3	Aileron	Sealed	δ_a	16	43	5(b) & 7

NATIONAL ADVISORY
COMMITTEE FOR AERONAUTICS.

TABLE II
WING AND FLAP CONFIGURATIONS

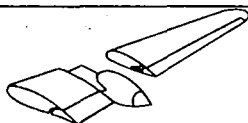
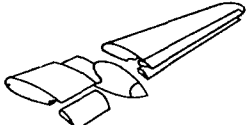
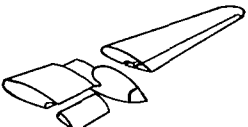
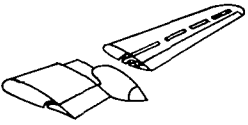
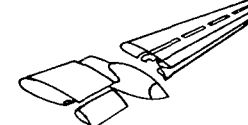
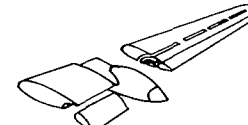

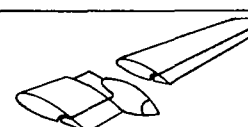
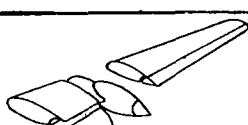


Wing	Symbol	Flap	δ_{r1} (deg)	δ_{r0} (deg)	δ_{rs} (deg)	Flight condition
CVAC original wing	W_1	full-span	0 20 40	0 50 50	----- ----- -----	Normal Take-off Landing
-----Do-----	W_1	partial-span, single-slot- ted	40	-----	-----	Landing
Original wing with slotted outer panels	W_2	full-span	0 20 40	0 50 50	----- ----- -----	Normal Take-off Landing
-----Do-----	W_2	partial-span, single-slot- ted	20 40	----- -----	----- -----	Take-off Landing
-----Do-----	W_2	partial-span, double-slot- ted	----- -----	----- -----	0 50	Normal Landing
Original wing wing NACA outer panels	W_3	partial-span, single-slot- ted	0 20 40	----- ----- -----	----- ----- -----	Normal Take-off Landing
-----Do-----	W_3	partial-span, double-slot- ted	----- -----	----- -----	0 50	Normal Landing

NATIONAL ADVISORY
COMMITTEE FOR AERONAUTICS.

TABLE III
LIST OF FIGURES

Figure No.	Type of Presentation	Model Wing	Remarks
1	3-view of the model	W ₁	Drawing
2	Details of midchord slot	W ₂	Do
3(a) & 3(b)	Close up of midchord slot	W ₂	Photograph
4	Rigging diagram and physical characteristics of the wing planforms	W ₁ , W ₂ , & W ₃	Drawing
5(a)	Details of flap and aileron arrangement	W ₁ & W ₂	Do
5(b)	-----Do-----	W ₃	Do
6(a) & 6(b)	Flap positions tested	W ₁ , W ₂ , & W ₃	Do
7	Comparison of sealed ailerons	-----do-----	Do
8	Model set-up in test section	W ₁	Photograph
9(a)	Stalling characteristics	W ₁	Normal flight and landing conditions; $T_0 = 0$; $R \approx 2,500,000$
9(b)	-----Do-----	W ₁	Normal flight condition; propellers removed; $R \approx 5,500,000$
10	Leading-edge spoiler installation	W ₁	Drawing
11(a)	Stalling characteristics	W ₁	Normal flight condition; rated power; spoilers off and on; $R \approx 2,500,000$
11(b)	-----Do-----	W ₁	Landing condition; 40-percent rated power; spoilers on and off; $R \approx 2,500,000$
12(a)	Aerodynamic characteristics of the model with leading-edge spoilers	W ₁	C_D , α , C_m , vs C_L ; normal flight condition; $R \approx 2,500,000$
12(b)	-----Do-----	W ₁	C_D , α , C_m , vs C_L ; landing condition; $R \approx 2,500,000$
13(a)	Stalling characteristics; full-span flaps	W ₂	Normal flight, take-off, and landing conditions; propellers off; $R \approx 4,500,000$
13(b)	Stalling characteristics; partial-span, single-slotted flaps	W ₂	Take-off and landing conditions; propellers off; $R \approx 4,500,000$
13(c)	Stalling characteristics; partial-span, double-slotted flaps	W ₂	Normal flight, and landing conditions; propellers off; $R \approx 4,500,000$
14	Stalling characteristics	W ₃	Do
15(a)	Aileron characteristics	W ₁	C_L , C_L , vs α ; normal flight condition; $R \approx 4,500,000$
15(b)	Aileron characteristics; full-span, single-slotted flaps	W ₁	C_L , C_L , vs α ; landing condition; $R \approx 4,500,000$
15(c)	Aileron characteristics; partial-span, single-slotted flaps	W ₁	Do
16	Estimated helix angle	W ₁	$\frac{p_b}{2V}$ vs V ; normal flight and landing conditions
17(a)	Aileron characteristics	W ₂	C_L , C_L , vs α ; normal flight condition; $R \approx 4,500,000$
17(b)	Aileron characteristics; full-span, single-slotted flaps	W ₂	C_L , C_L , vs α ; landing condition; $R \approx 4,500,000$
17(c)	Aileron characteristics; partial-span, single-slotted flaps	W ₂	Do
17(d)	Aileron characteristics; partial-span, double-slotted flaps	W ₂	Do
18	Estimated helix angle	W ₂	$\frac{p_b}{2V}$ vs V ; normal flight and landing conditions
19(a)	Aileron characteristics	W ₃	C_L , C_L , vs α ; normal flight condition; $R \approx 4,500,000$
19(b)	Aileron characteristics; partial-span, double-slotted flaps	W ₃	C_L , C_L , vs α ; landing condition; $R \approx 4,500,000$
20	Estimated helix angle	W ₃	$\frac{p_b}{2V}$ vs V ; normal flight and landing conditions

CONFIDENTIAL		TABLE III (Concluded)	NATIONAL ADVISORY COMMITTEE FOR AERONAUTICS
Figure No.	Type of Presentation	Model Wing	Remarks
21(a) & 21(b)	Details of transition strips	W ₃	Photograph
22(a)	Aerodynamic characteristics; full- and partial-span; single-slotted flaps	W ₁	C _D , α , C _m , vs C _L ; normal flight, take-off, and landing conditions; $R \approx 4,500,000$
22(b)	Aerodynamic characteristics; full-span, single-slotted flaps; fixed transition	W ₁	C _D , α , C _m , vs C _L ; normal flight and landing conditions; $R \approx 4,500,000$
23(a)	Aerodynamic characteristics; full-span and partial-span, single-slotted flaps	W ₂	C _D , α , C _m , vs C _L ; normal flight, take-off, and landing conditions; $R \approx 4,500,000$
23(b)	Aerodynamic characteristics; partial-span, double-slotted flaps	W ₂	C _D , α , C _m , vs C _L ; normal flight and landing conditions; $\delta_e = 0^\circ$ and -10° ; $R \approx 4,500,000$
24(a)	Aerodynamic characteristics; partial-span, single-slotted flaps	W ₃	C _D , α , C _m , vs C _L ; normal flight, take-off, and landing conditions; $R \approx 4,500,000$
24(b)	Aerodynamic characteristics; partial-span, double-slotted flaps; natural and fixed transition	W ₃	C _D , α , C _m , vs C _L ; normal flight and landing conditions; $\delta_e = 0^\circ$ and -10° ; $R \approx 4,500,000$
25(a) & 25(b)	Details of flap-nacelle seals	W ₃	Photograph
26	Aerodynamic characteristics; full- and modified flap-nacelle seals	W ₃	C _D , α , C _m , vs C _L ; landing condition; $R \approx 4,500,000$
27	Spanwise section-lift-coefficient distribution	W ₁	C _L vs y ; normal flight condition
28	-----DO-----	W ₃	Do

TABLE IV - SUMMARY OF RESULTS AT $R \approx 4,500,000$												
NATIONAL ADVISORY COMMITTEE FOR AERONAUTICS.												
Model Configuration	Wing	Flap deflection (deg)			$C_{l_{max}}$	α at $C_{l_{max}}$ (deg)	$C_{l_{cm=0}}$	C_D		$\frac{pb}{2V}$ at 1.1V _s		Figure No.
		δ_{r_1}	δ_{r_0}	δ_{r_s}				$C_{L=0.4}$	$C_{L=0.8}$	$\alpha = +20$ -25	$\alpha = +20$ -25	
	W ₁	0	0	---	1.33	19.0	1.01	0.026	0.040	----	0.060	15(a), 16, & 22(a)
	W ₁	20	50	---	1.75	13.3	1.08	----	.098	----	----	22(a)
	W ₁	40	50	---	1.99	11.5	1.37	----	----	----	.031	15(b), 16, & 22(a)
	W ₁	40	---	---	1.95	18.4	1.54	.102	.108	----	.051	15(c), 16, & 22(a)
	W ₂	0	0	---	1.38	18.1	1.05	.030	.043	----	.062	17(a), 18, & 23(a)
	W ₂	20	50	---	1.86	16.0	1.10	----	.099	----	----	23(a)
	W ₂	40	50	---	2.12	14.6	1.38	----	----	----	.039	17(b), 18, & 23(a)
	W ₂	40	---	---	2.04	15.6	1.50	.105	.113	----	.053	17(c), 18, & 23(a)
	W ₂	---	---	50	2.24	15.7	1.85	----	----	0.070	.063	17(d), 18, & 23(b)
	W ₃	---	---	0	1.35	21.1	1.05	----	----	.076	.069	19(a), 20, & 24(a)
	W ₃	---	---	---	*1.40	---	*1.11	*.028	*.042	---	---	---
	W ₃	20	---	---	1.63	16.3	1.44	----	----	----	----	24(a)
	W ₃	40	---	---	*1.69	16.6	*1.51	*.064	*.073	----	----	24(a)
	W ₃	---	---	50	1.88	---	*1.75	----	----	----	----	19(b), 20, & 24(b)
	W ₃	---	---	---	*1.95	---	---	----	----	*.115	----	---
	W ₃	---	---	50	2.10	16.8	1.88	----	----	.076	.063	19(b), 20, & 24(b)
					*2.15	---	*1.91	----	----	----	----	---

*Coefficients based on area of W_1

NATIONAL ADVISORY
COMMITTEE FOR AERONAUTICS.

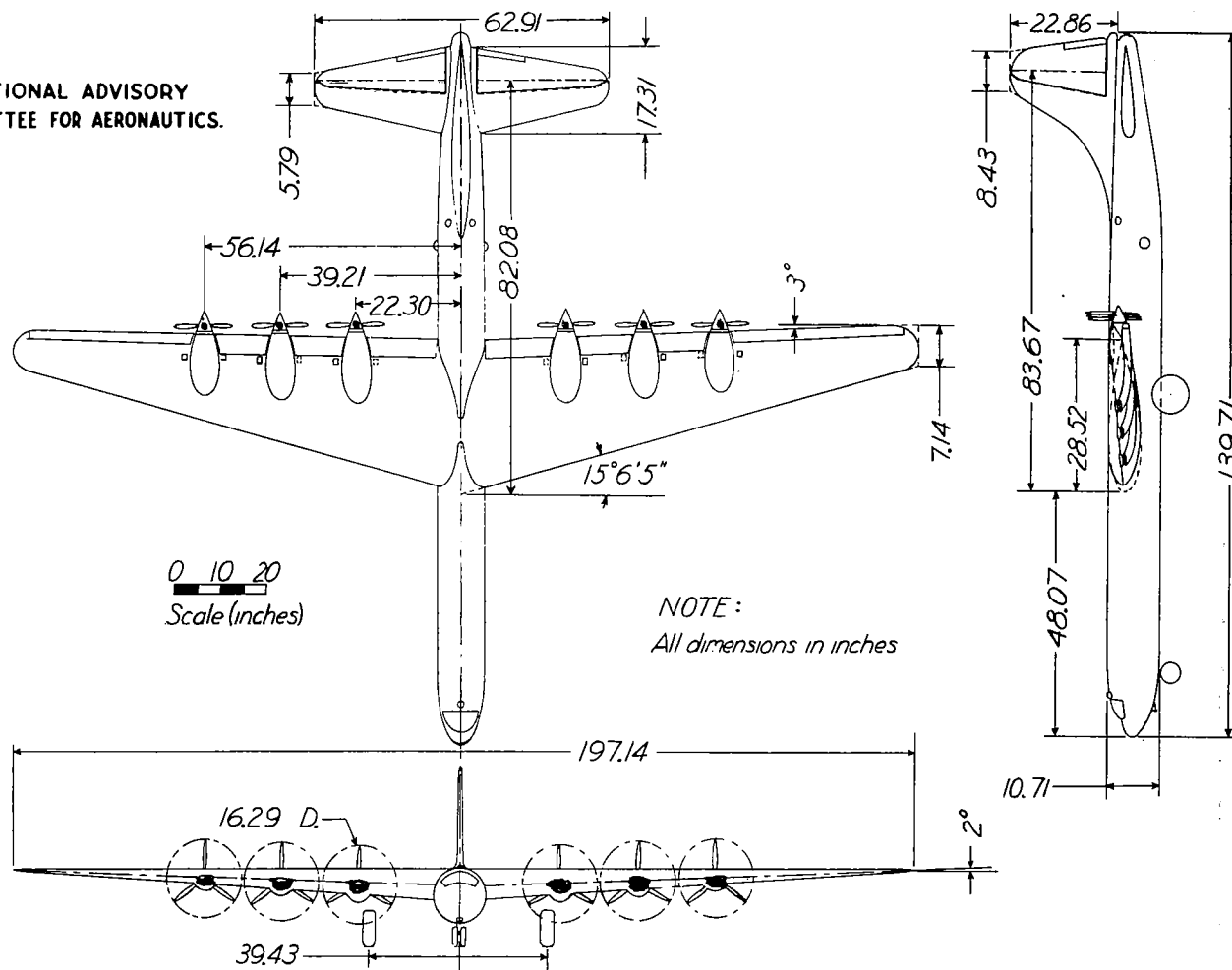
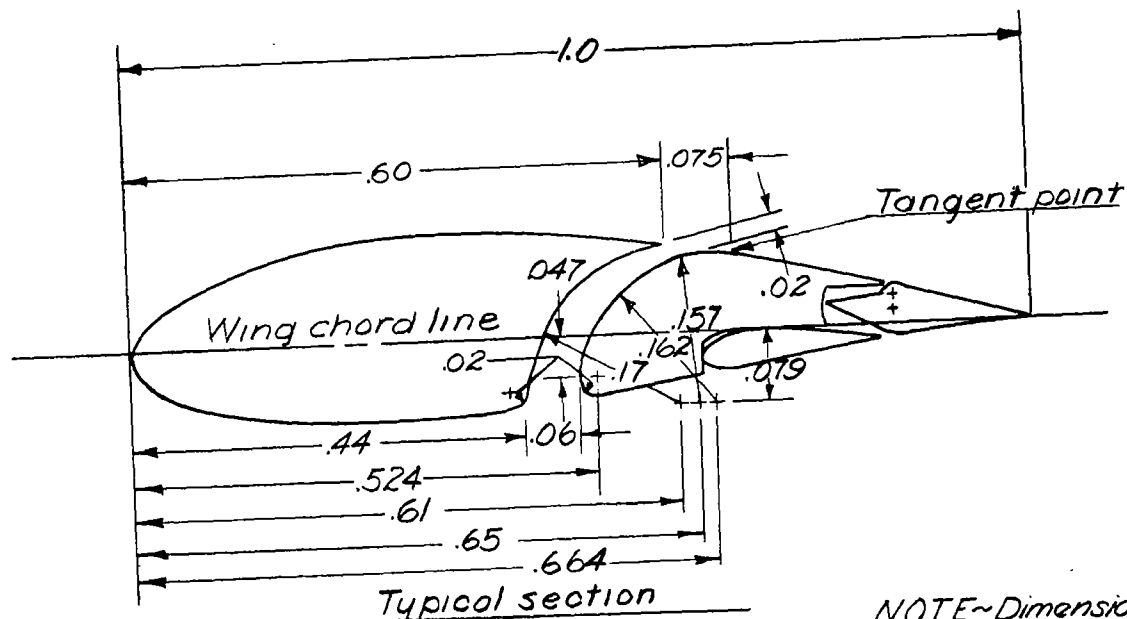


Figure 1.-Three-view drawing of a 1/14-scale model of the XB-36 airplane. Wing W_f.



NOTE~Dimensions in fraction of wing section chord.

NATIONAL ADVISORY
COMMITTEE FOR AERONAUTICS.

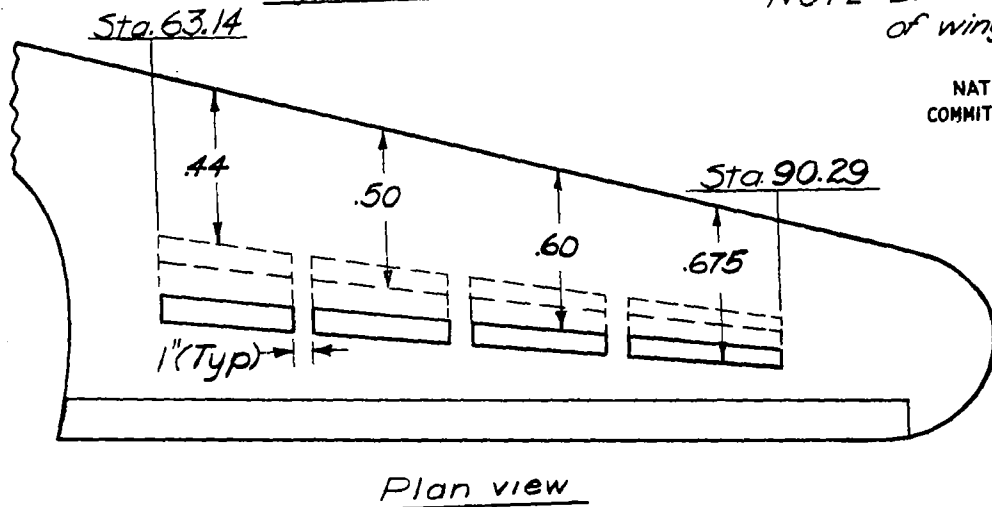
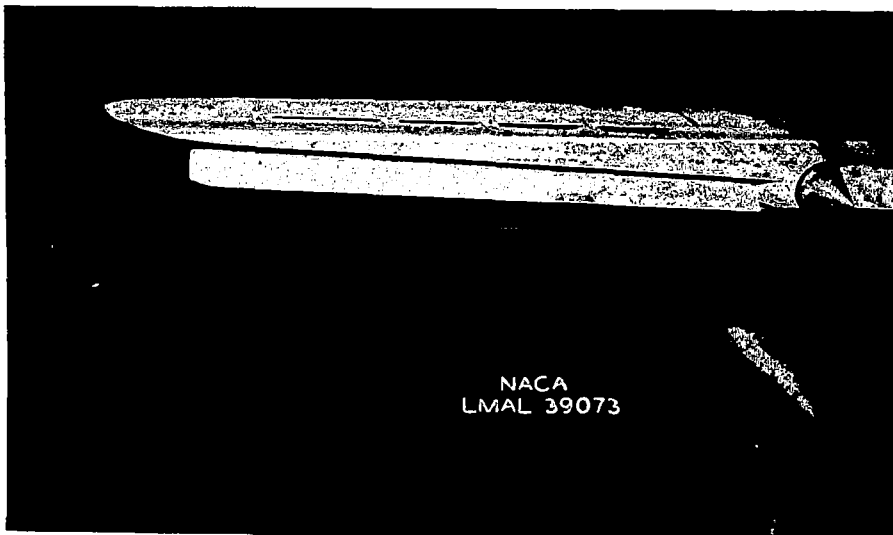
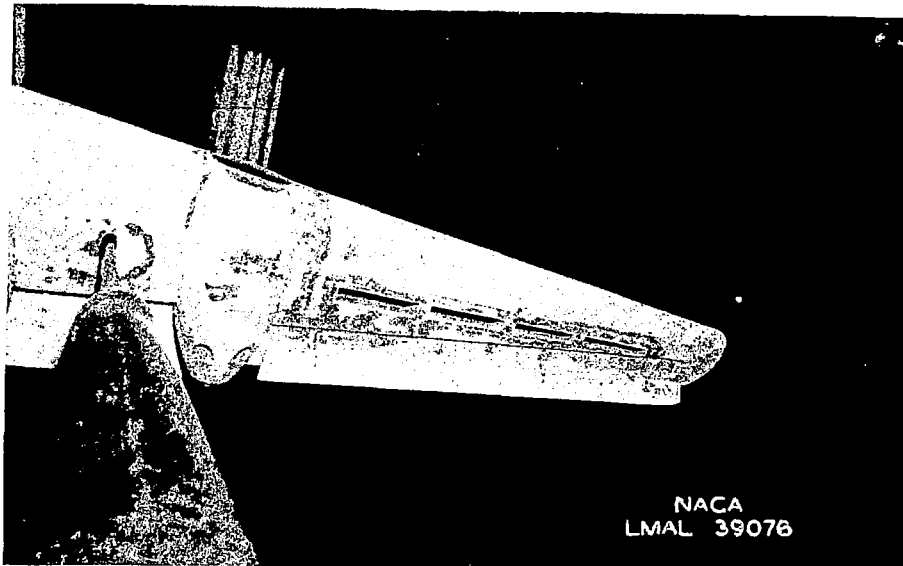


Figure 2. — Midchord slot installation; $1/14$ -scale model of the XB-36 airplane.



(a) Wing upper surface.



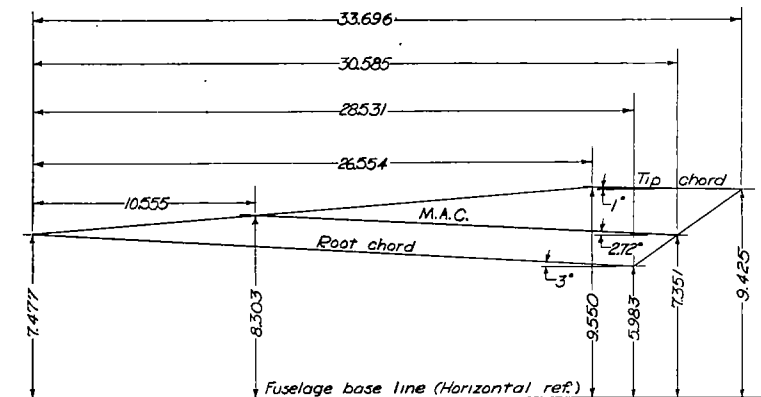
(b) Wing lower surface.

Figure 3.- Midchord slot; $\frac{1}{14}$ -scale model of the XB-36 airplane.

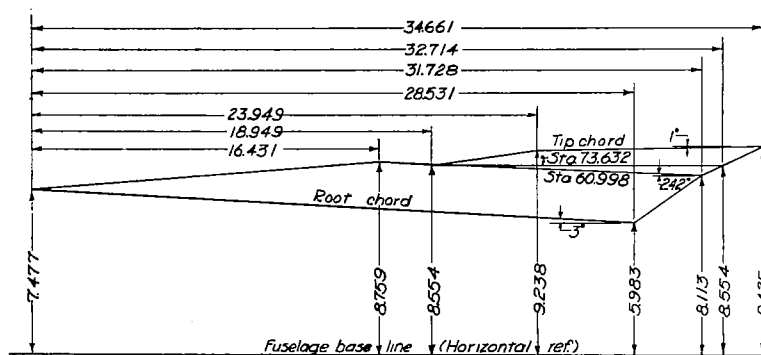
NATIONAL ADVISORY
COMMITTEE FOR AERONAUTICS.

~ Model Wing Data ~

	$W_1, \xi W_2$	W_3
Airfoil section-		
root	NACA 63(420)-422	NACA 63(420)-422
tip	NACA 63(420)517	NACA 65(345)-517
Area (sq. ft.)	24.347	25.281
Span	197.142	197.142
Root chord	28.531	28.531
Tip chord	7.142	10.712
Mean aerodynamic chord (MAC)	20.050	20.241
Sweepback of L.E. (outbd of Sta 60.998)	15° 6' 5"	11° 21'
Sweepback of T.E. (outbd of Sta 60.998)	3°	4° 27' 36"
Taper ratio	4.000	2.666
Dihedral (from wingroot chord plane)	2°	2°
Angle of incidence at wing root chord	3°	3°
Root thickness (% root chord)	22	22
Tip thickness (% tip chord)	17	17
Aspect ratio	11.085	10.676



Rigging diagram- $W_1, \xi W_2$



Rigging diagram- W_3



NOTE~ All dimensions are given in inches

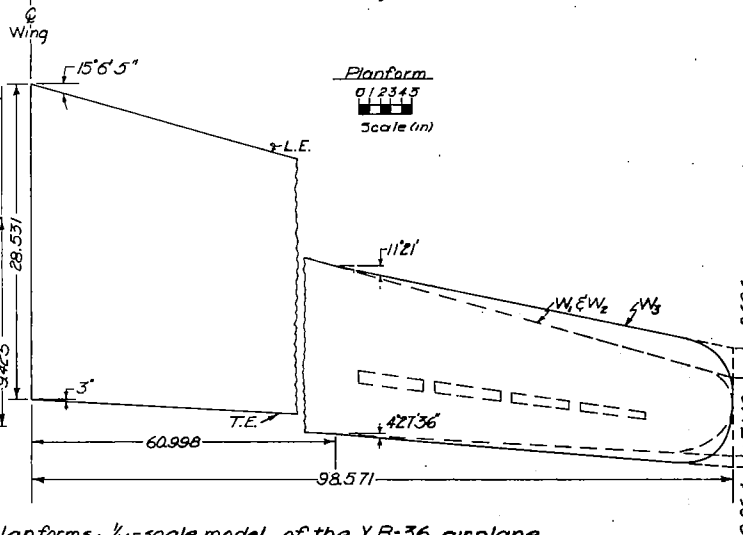


Figure 4.- Comparison of physical characteristics of two wing planforms; $1/4$ -scale model of the XB-36 airplane.

NATIONAL ADVISORY
COMMITTEE FOR AERONAUTICS.



NOTE~All dimensions are given in inches

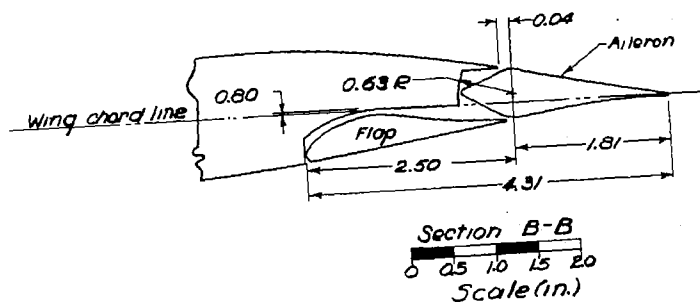
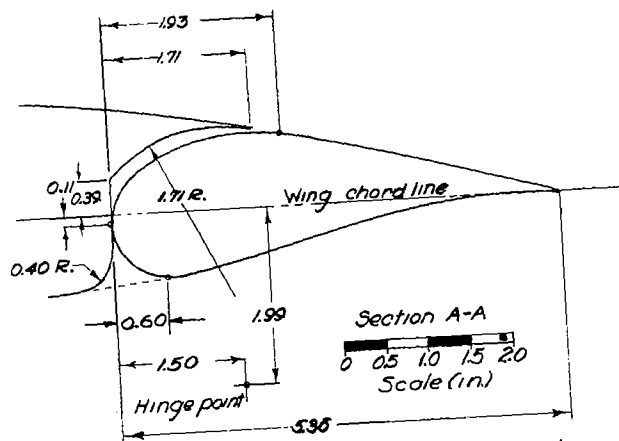
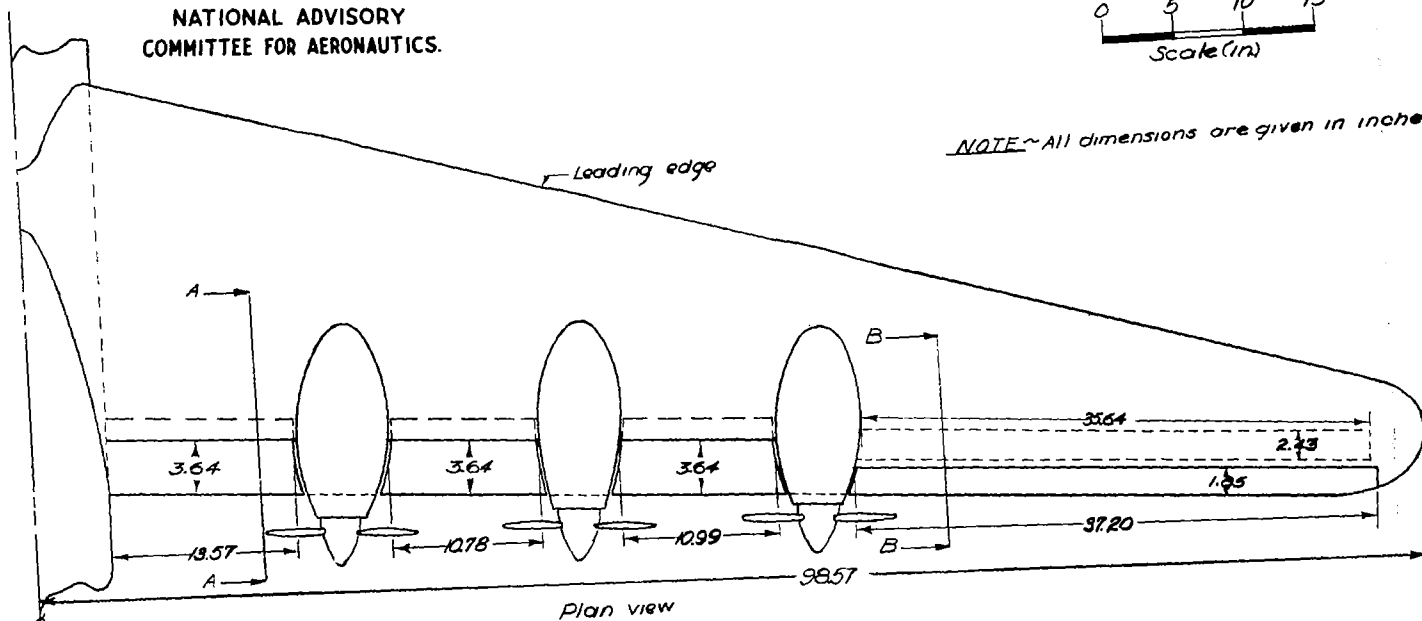
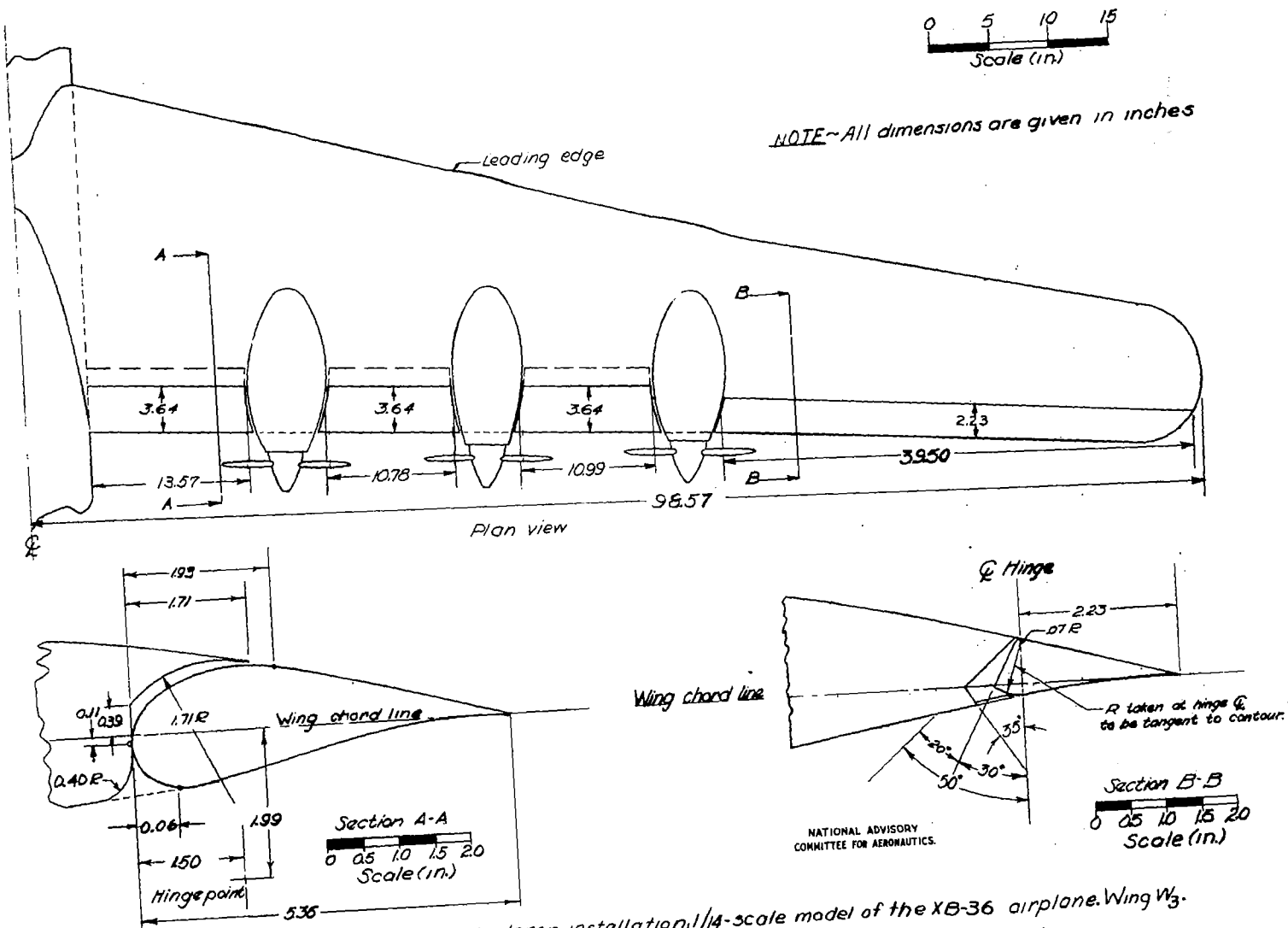
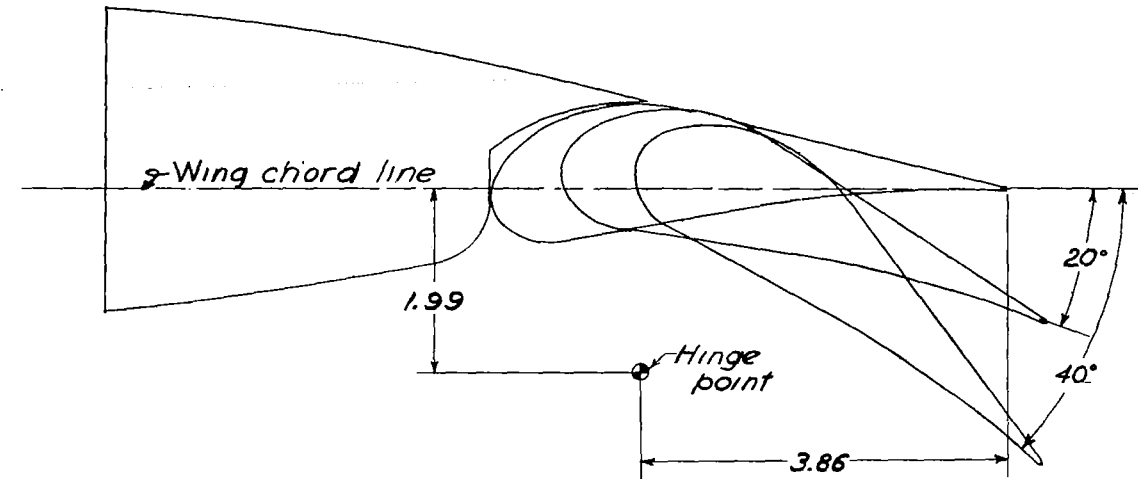
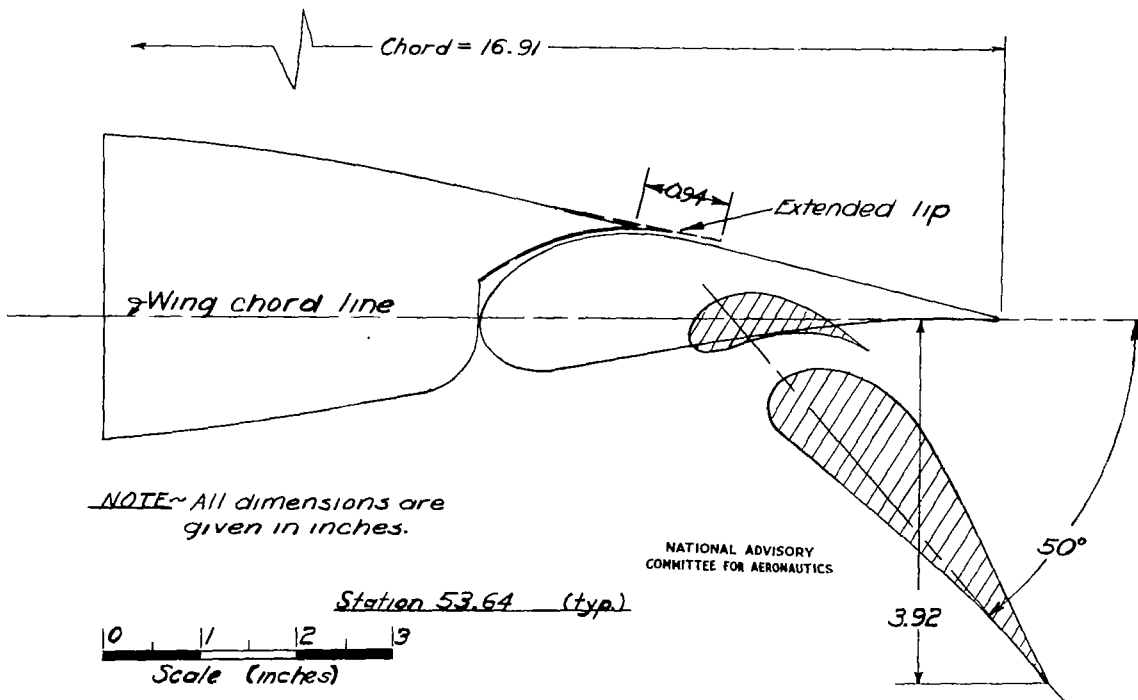


Figure 5(a).- Plan and section views of flap and aileron installation, 1/4-scale model of the XB-36 airplane. Wing W.



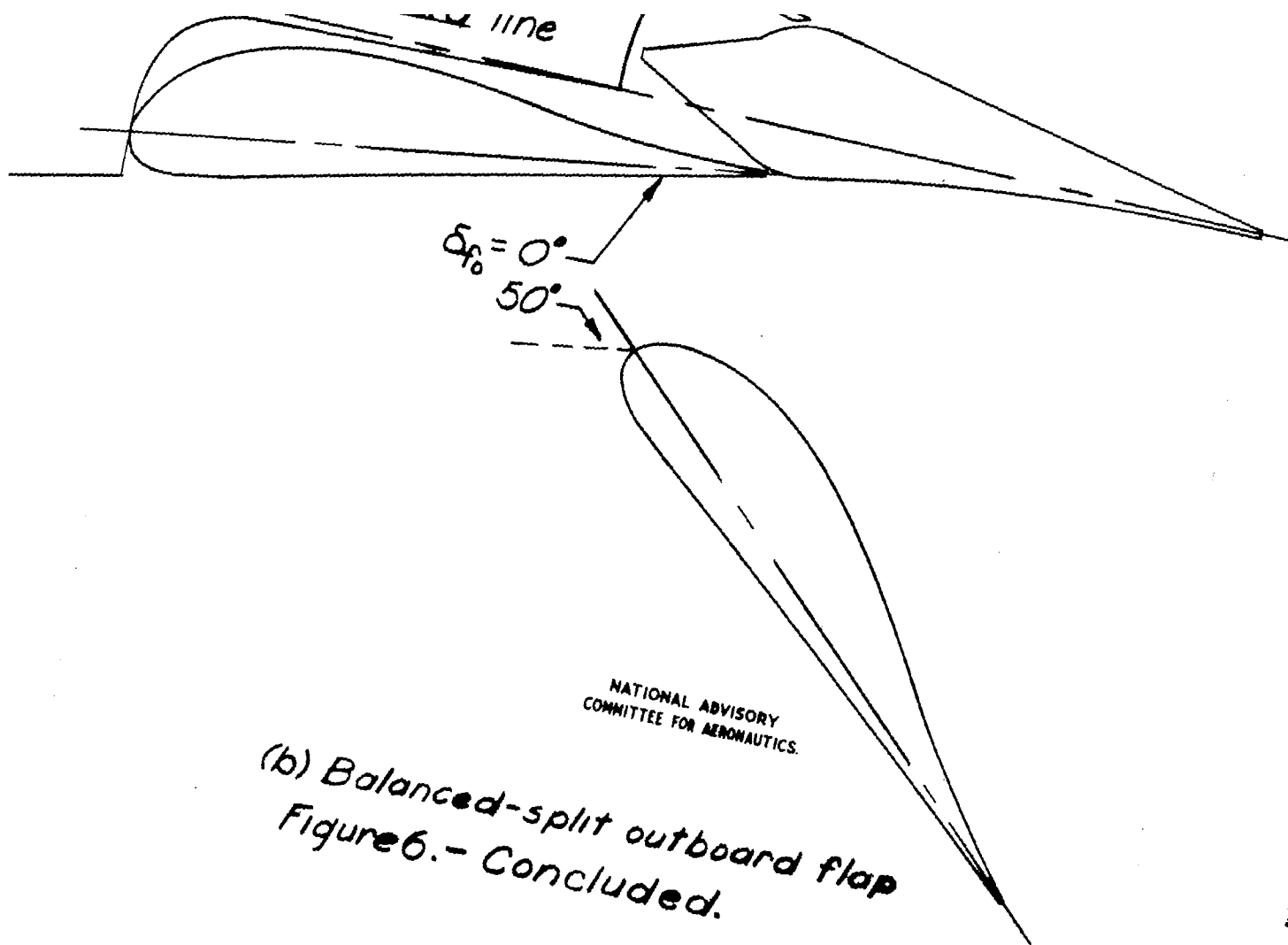


Station 53.64 (typ.)



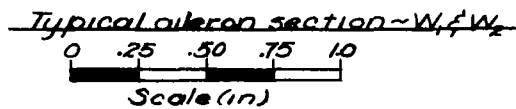
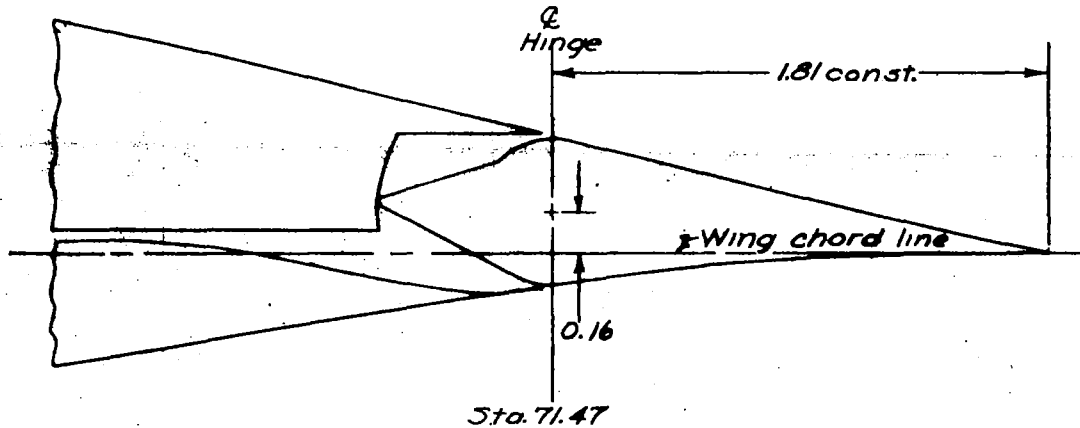
(a) Single- and double-slotted inboard flaps.

Figure 6.- Flap positions tested; 1/14-scale model of the XB-36 airplane.

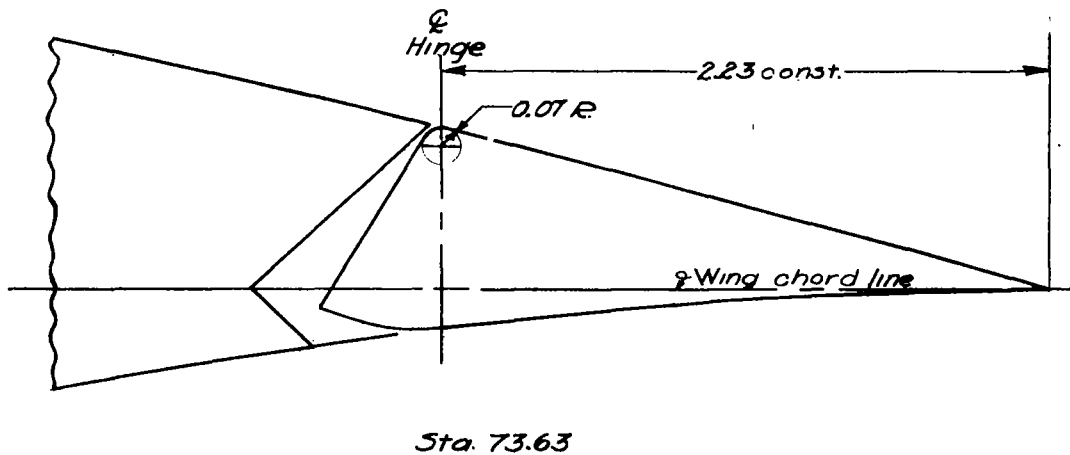


NATIONAL ADVISORY
COMMITTEE FOR AERONAUTICS.

(b) Balanced-split outboard flap
Figure 6.- Concluded.



NOTE~ All dimensions are given in inches



NATIONAL ADVISORY
COMMITTEE FOR AERONAUTICS.

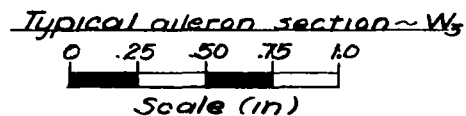


Figure 7.- Comparison of sealed ailerons used in tests of a 1/14-scale model of the XB-36 airplane.

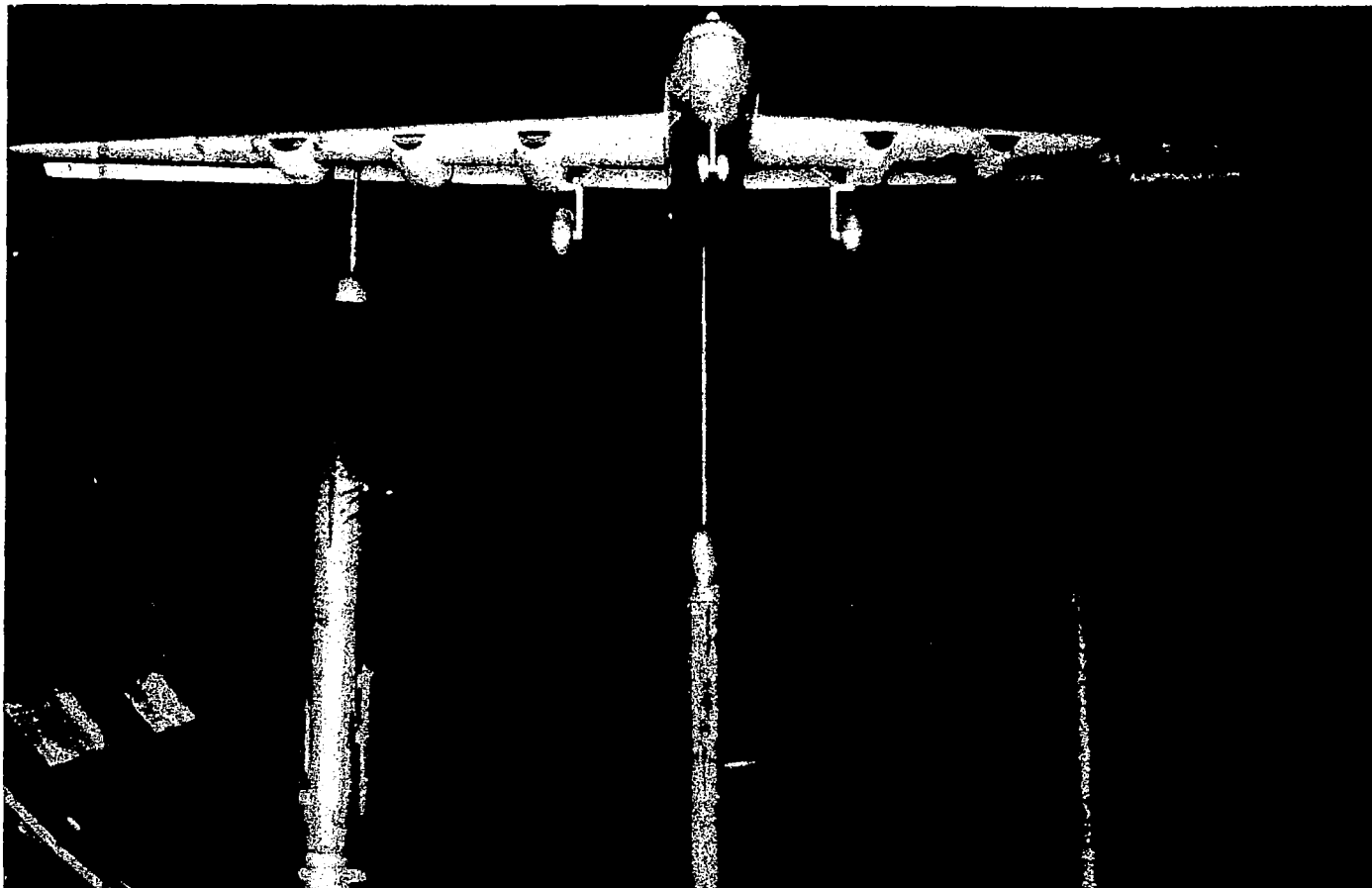
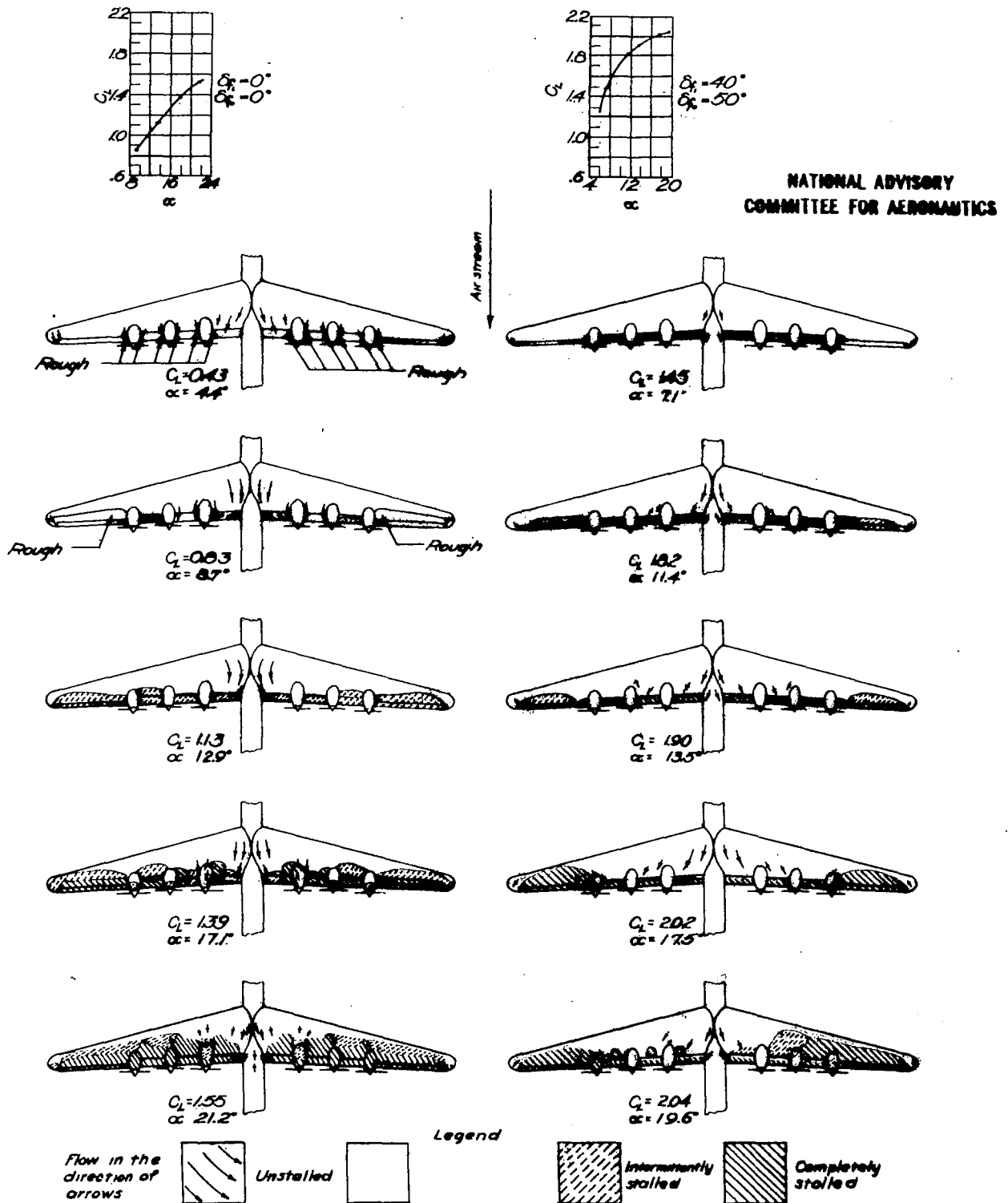


Figure 8.- A $\frac{1}{14}$ -scale model of the XB-36 airplane mounted on the normal supports in the test section of the Langley 19-foot pressure tunnel.



(a) Zero thrust; $R \approx 2,500,000$; $M = 0.09$.

Figure 9.—Stall studies of a 1/4-scale model of the XB-36 airplane. Wing W_1 ; original tail.

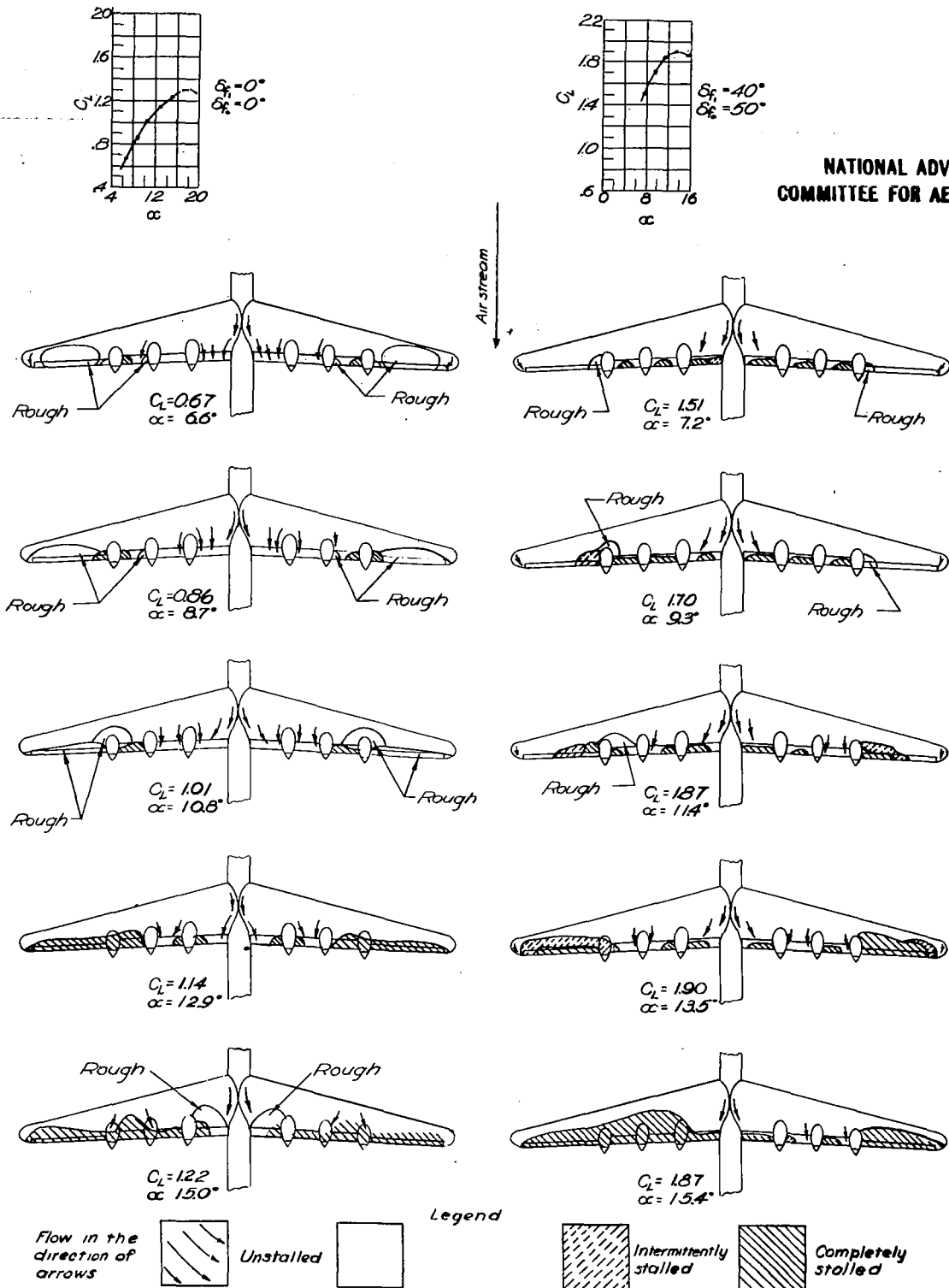
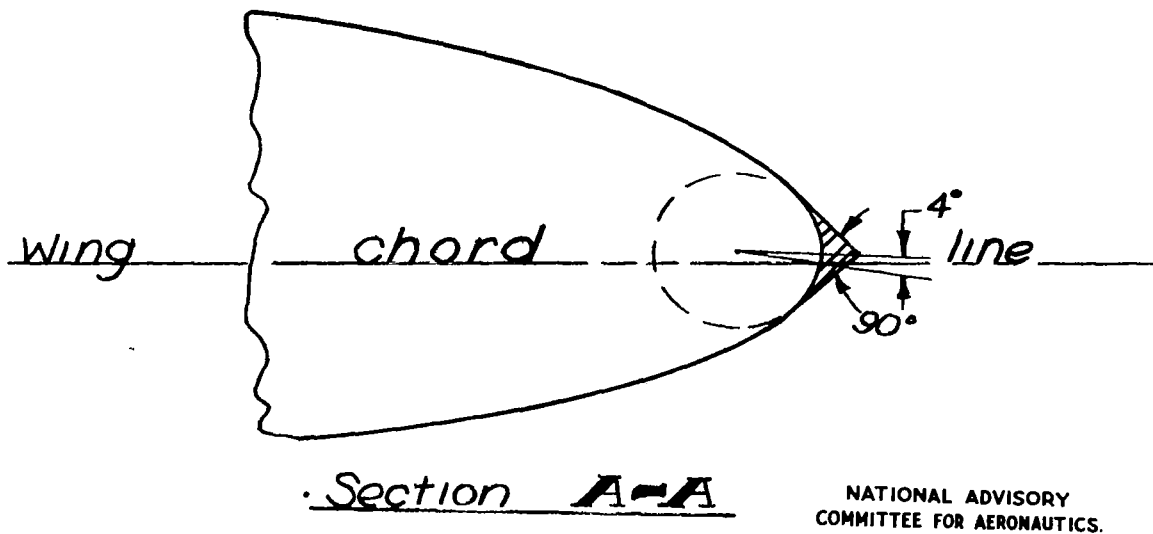
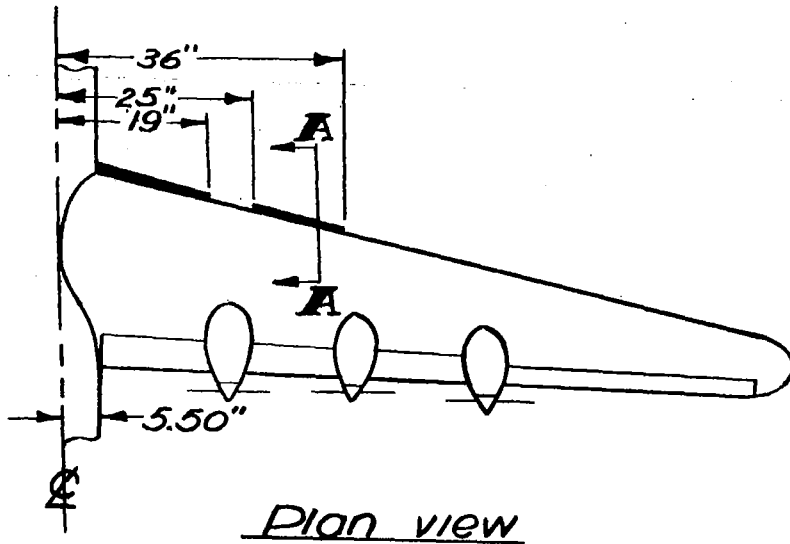
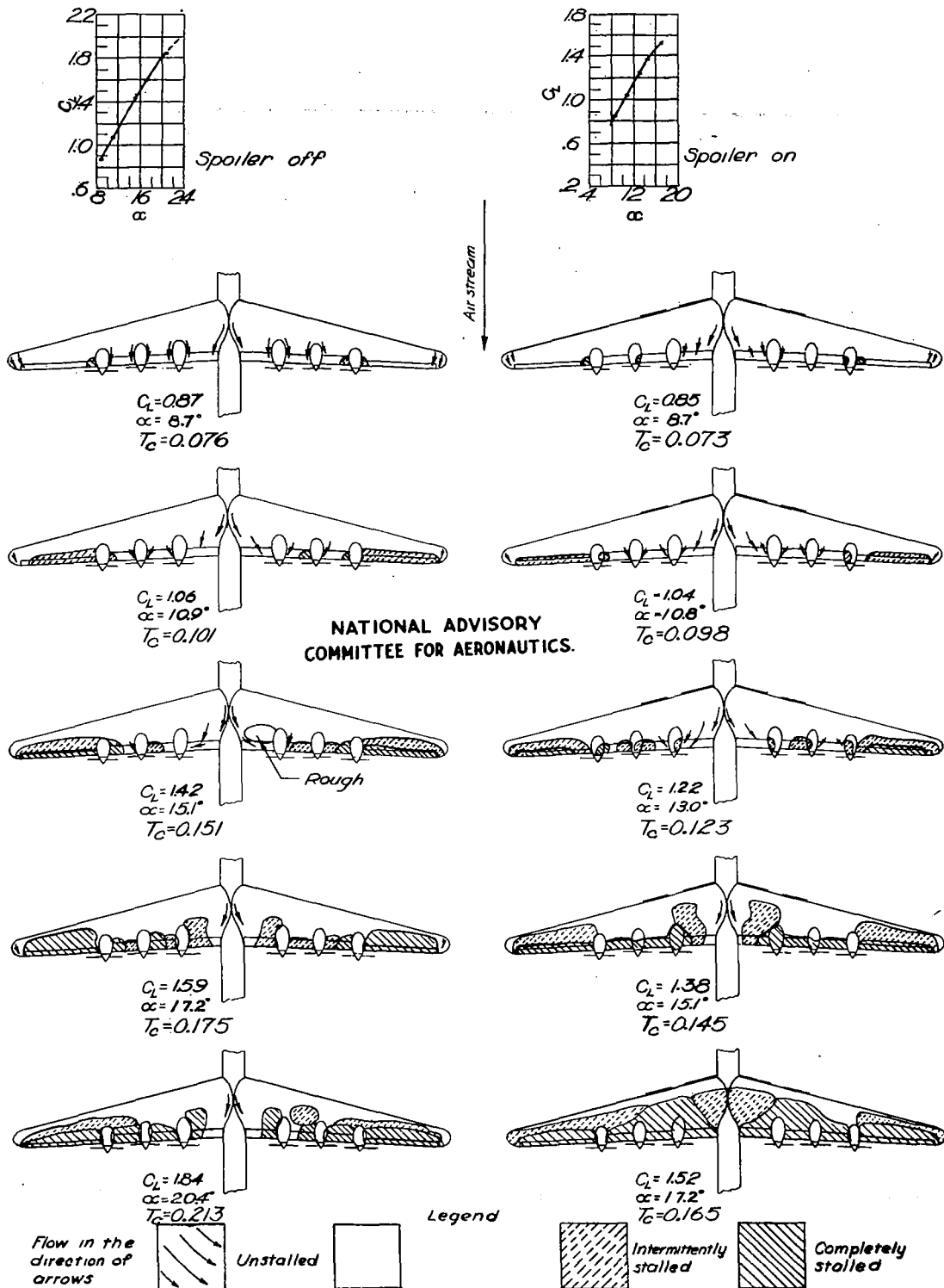
NATIONAL ADVISORY
COMMITTEE FOR AERONAUTICS(b) Propellers removed; $R \approx 5,500,000$; $M = 0.20$.

Figure 9 .- Concluded.

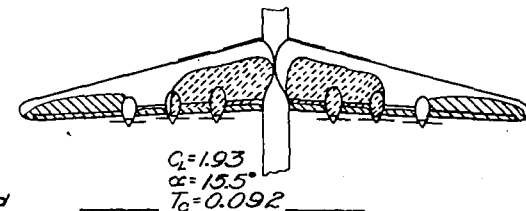
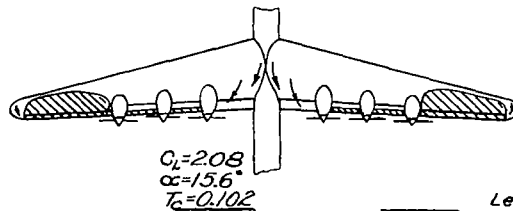
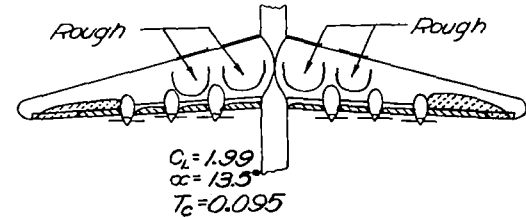
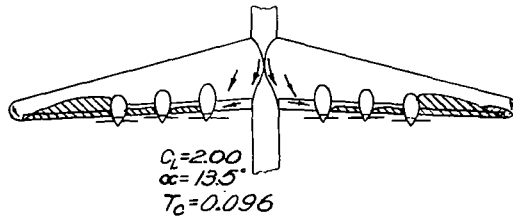
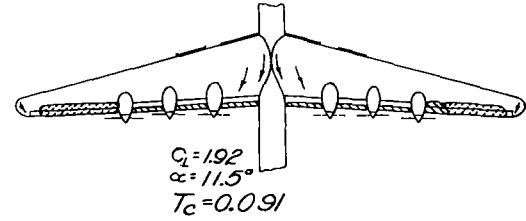
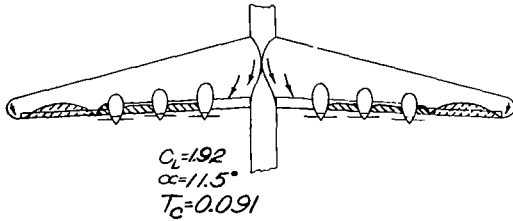
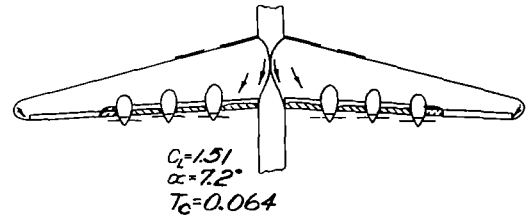
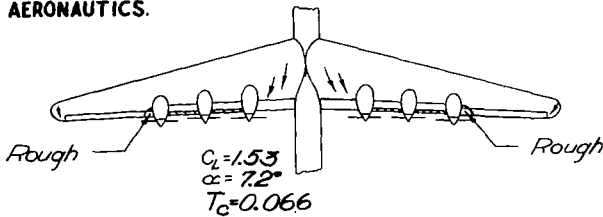
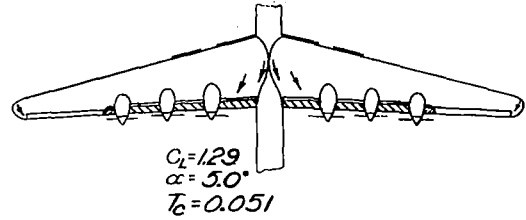
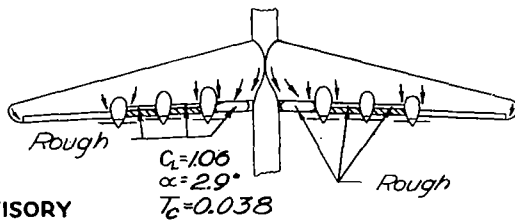
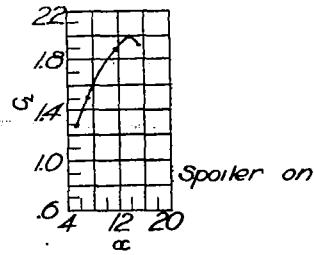
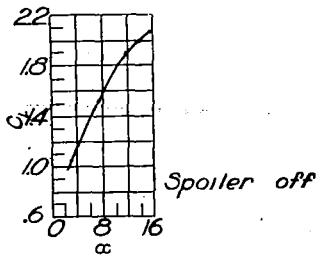


NATIONAL ADVISORY
COMMITTEE FOR AERONAUTICS.

Figure 10.— Plan and section views of a leading-edge spoiler arrangement; 1/14-scale model of the XB-36 airplane.



(a) $\delta_f = 0^\circ$; $\delta_p = 0^\circ$; Rated power @ S.L.; $R \approx 2,500,000$; $M = 0.09$.
Figure 11.- Effect of a leading-edge spoiler on the stall progression of a 1/14-scale model of the XB-36 airplane. Wing W_1 ; original tail.



Flow in the
direction of
arrows

Unstalled

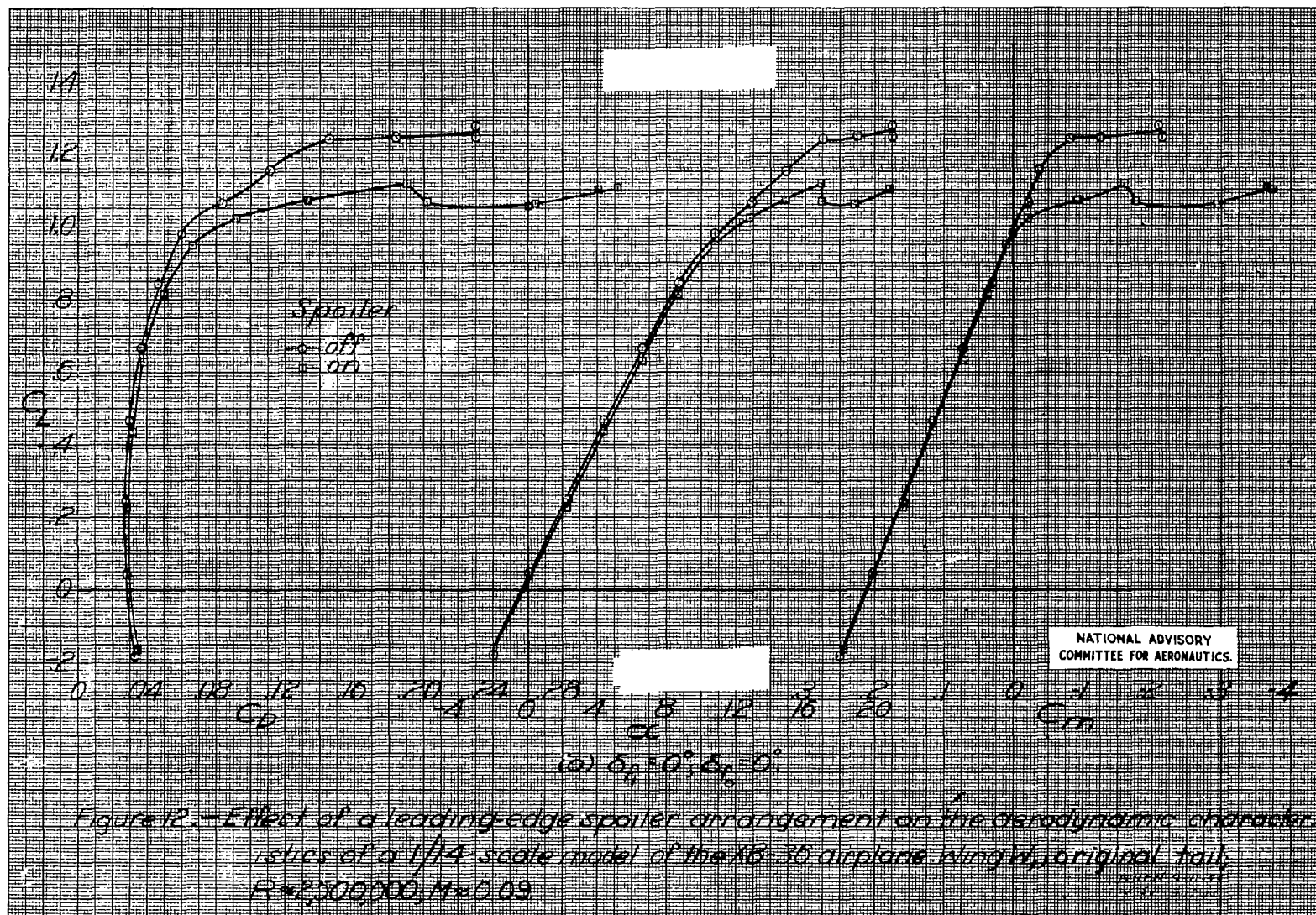
Legend

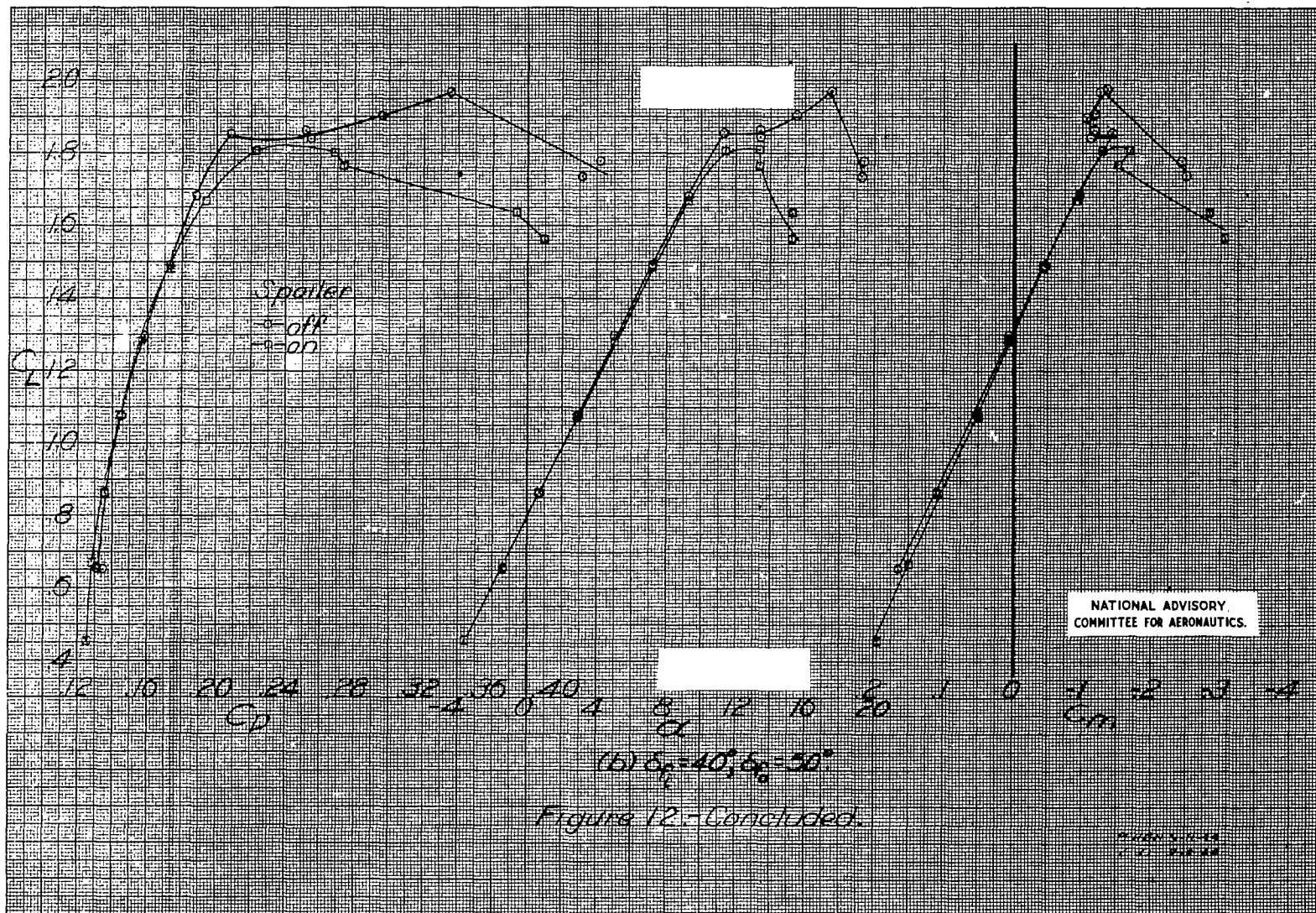
Legend

Intermittently
stalled

Completely
stalled

(b) $\delta_{fl} = 4.7^\circ$; $\delta_{fl} = 50^\circ$; 40% Rated power @ S. L.; $R \approx 2,500,000$; $M = 0.09$.
 Figure 11 - Concluded.





NATIONAL ADVISORY
COMMITTEE FOR AERONAUTICS.

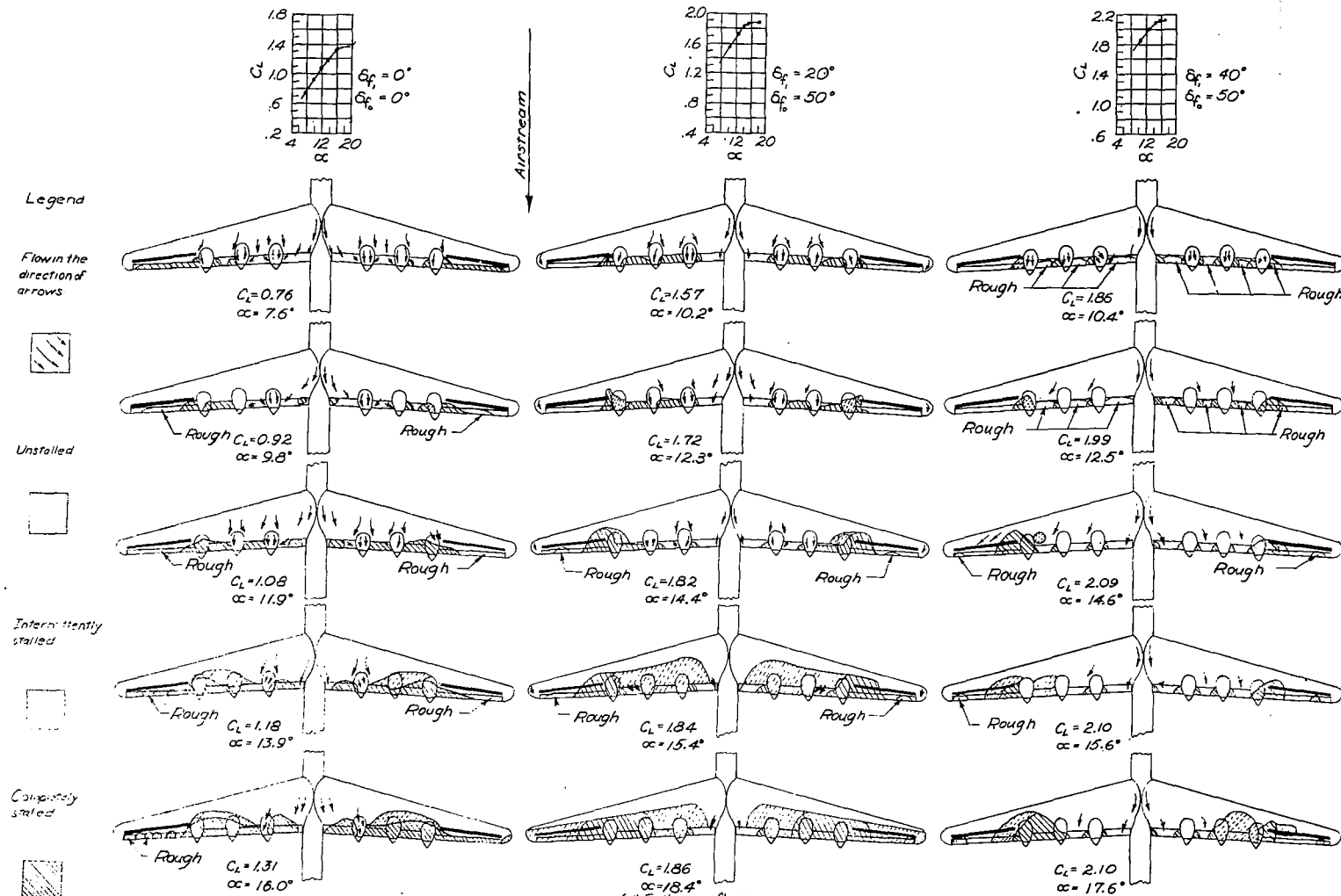
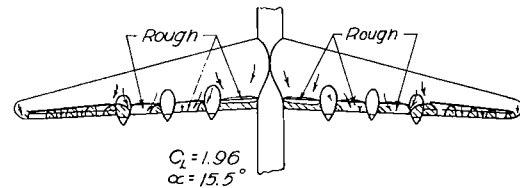
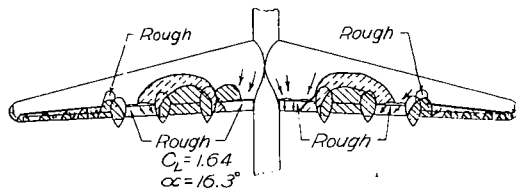
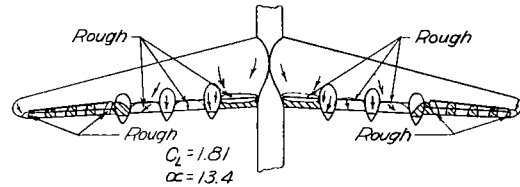
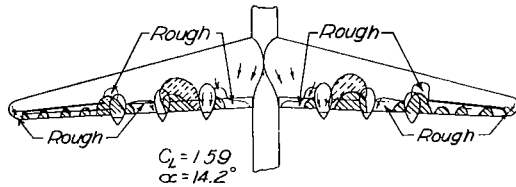
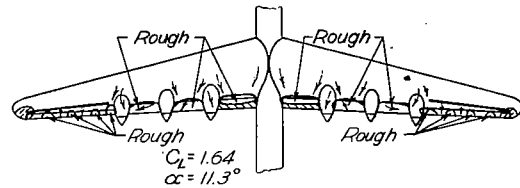
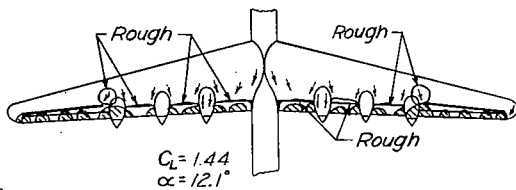
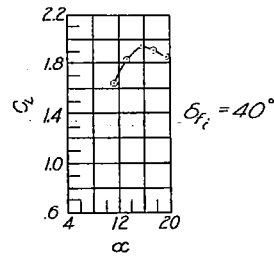
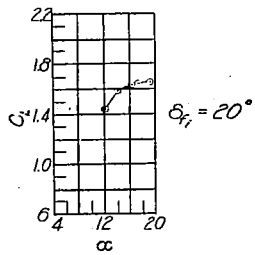
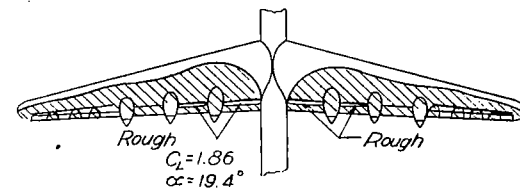
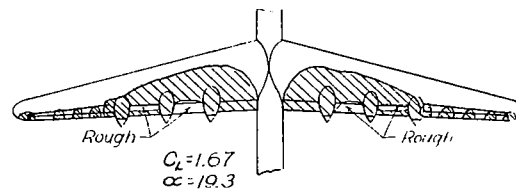
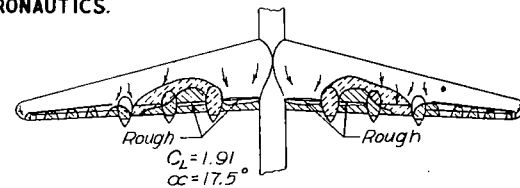
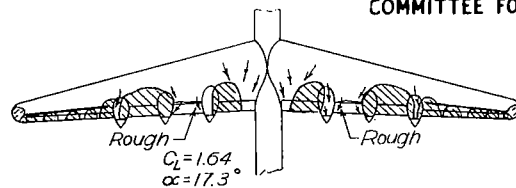


Figure 13. - Stall studies of a 1/14-scale model of the XB-36 airplane; Wing W_2 , $R \approx 4,500,000$, $M \approx 0.17$



NATIONAL ADVISORY
COMMITTEE FOR AERONAUTICS.



Flow in the
direction of
arrows



Unstalled



Legend

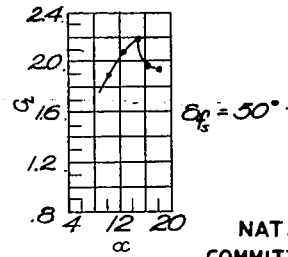
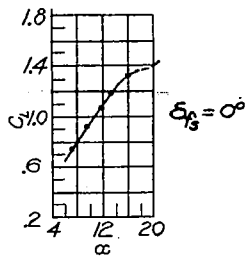


Intermittently
stalled

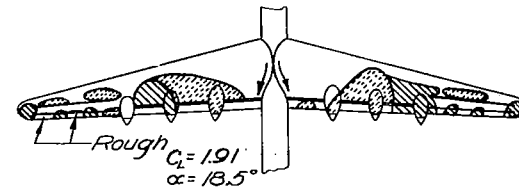
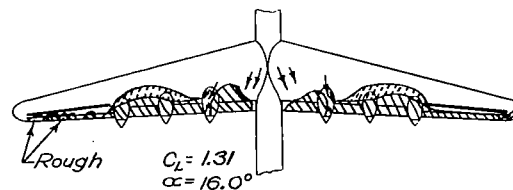
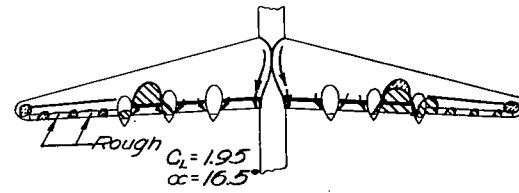
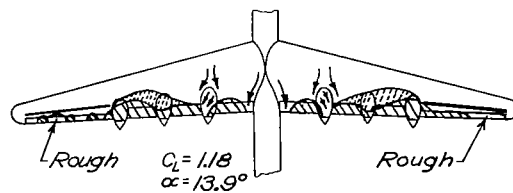
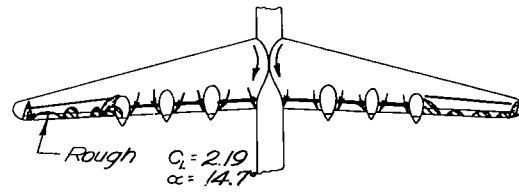
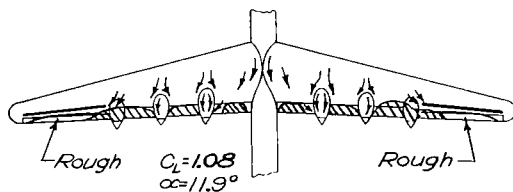
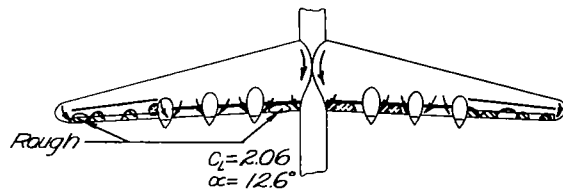
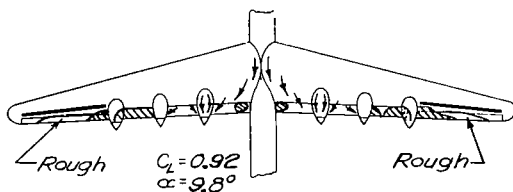
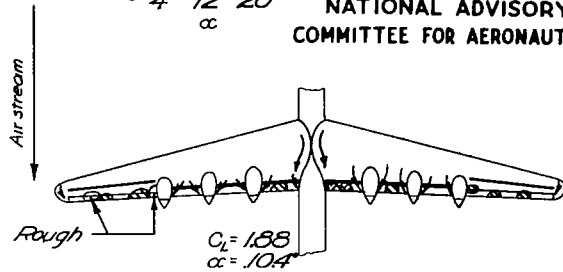
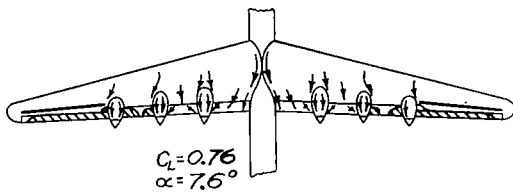


Completely
stalled

(b) Partial-span, single-slotted flaps.
Figure 13. - Continued.



NATIONAL ADVISORY
COMMITTEE FOR AERONAUTICS.



Flow in the
direction of
arrows



Unstalled



Legend

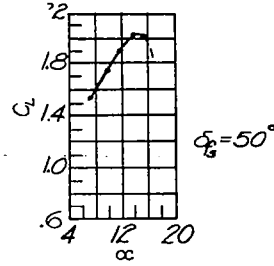
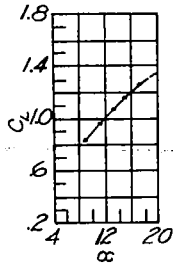


Intermittently
stalled

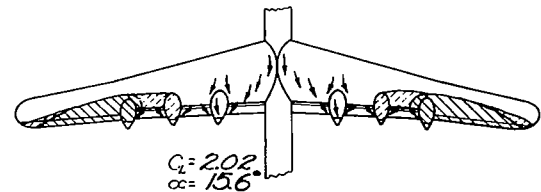
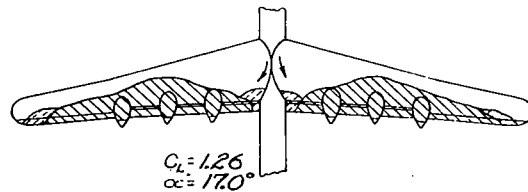
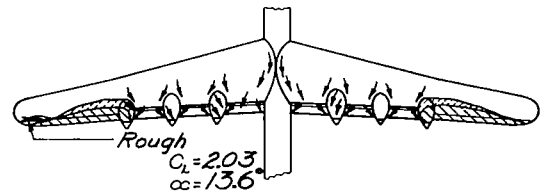
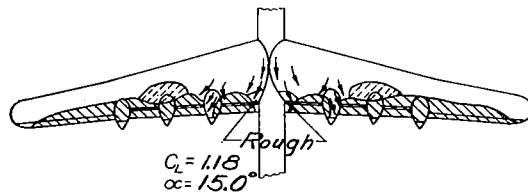
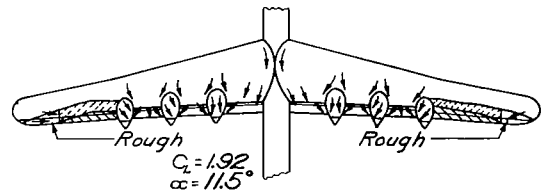
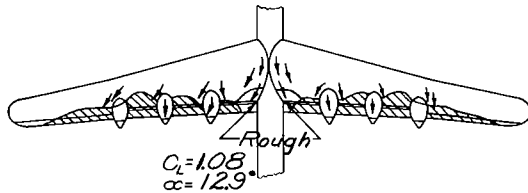
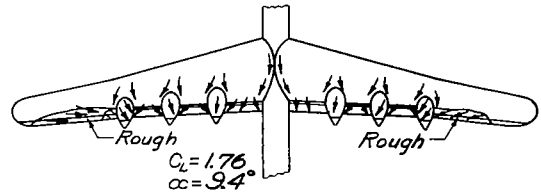
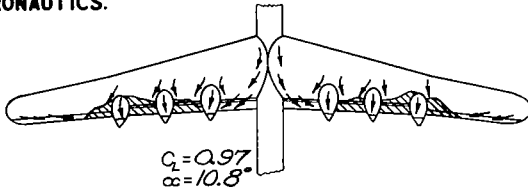
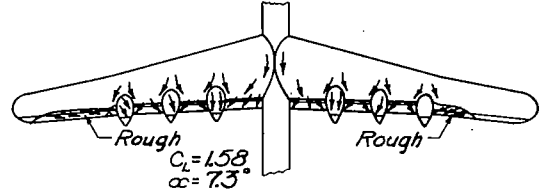
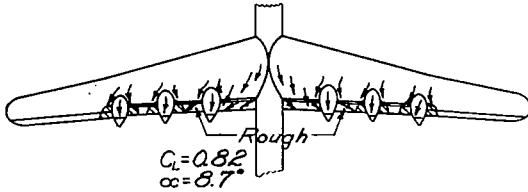


Completely
stalled

(c) Partial-span, double-slotted flaps.
Figure 13 - Concluded.



Airstream

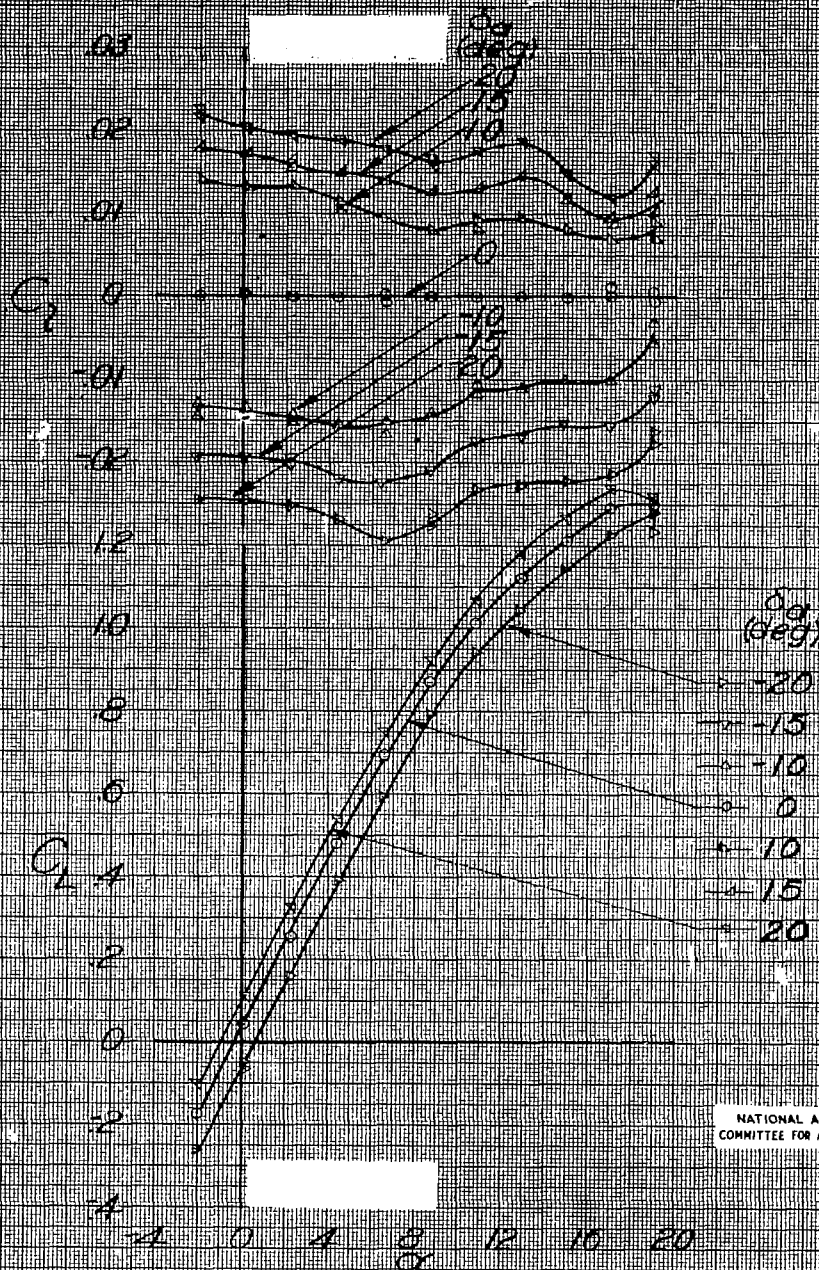
Flow in the
direction of
arrows

Unstalled



Legend

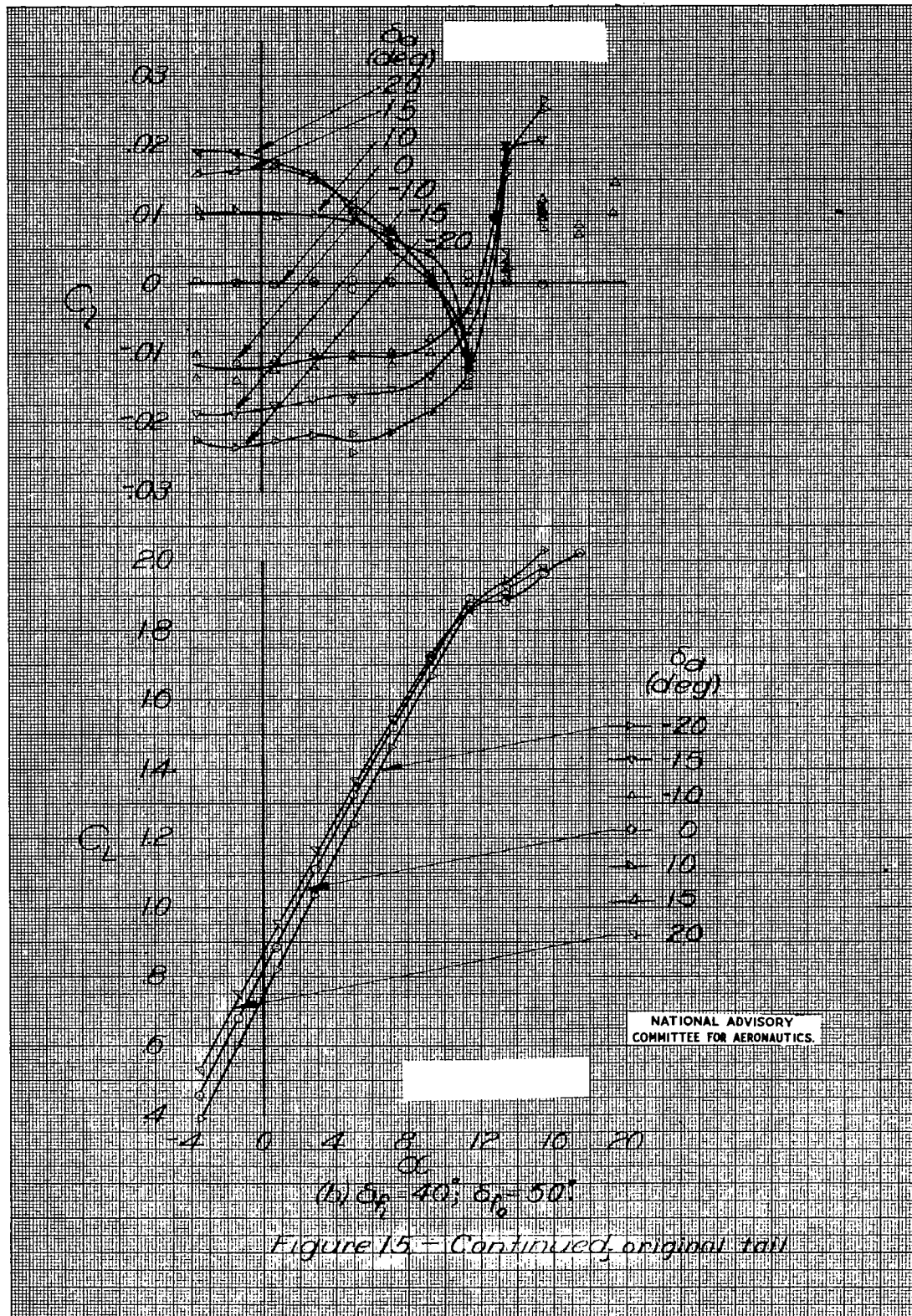
Intermittently
stalledCompletely
stalledFigure 14 - Stall studies of a 1/14-scale model of the XB-36 airplane. Wing W_3 , $R \approx 4,500,000$; $M \approx 0.17$.

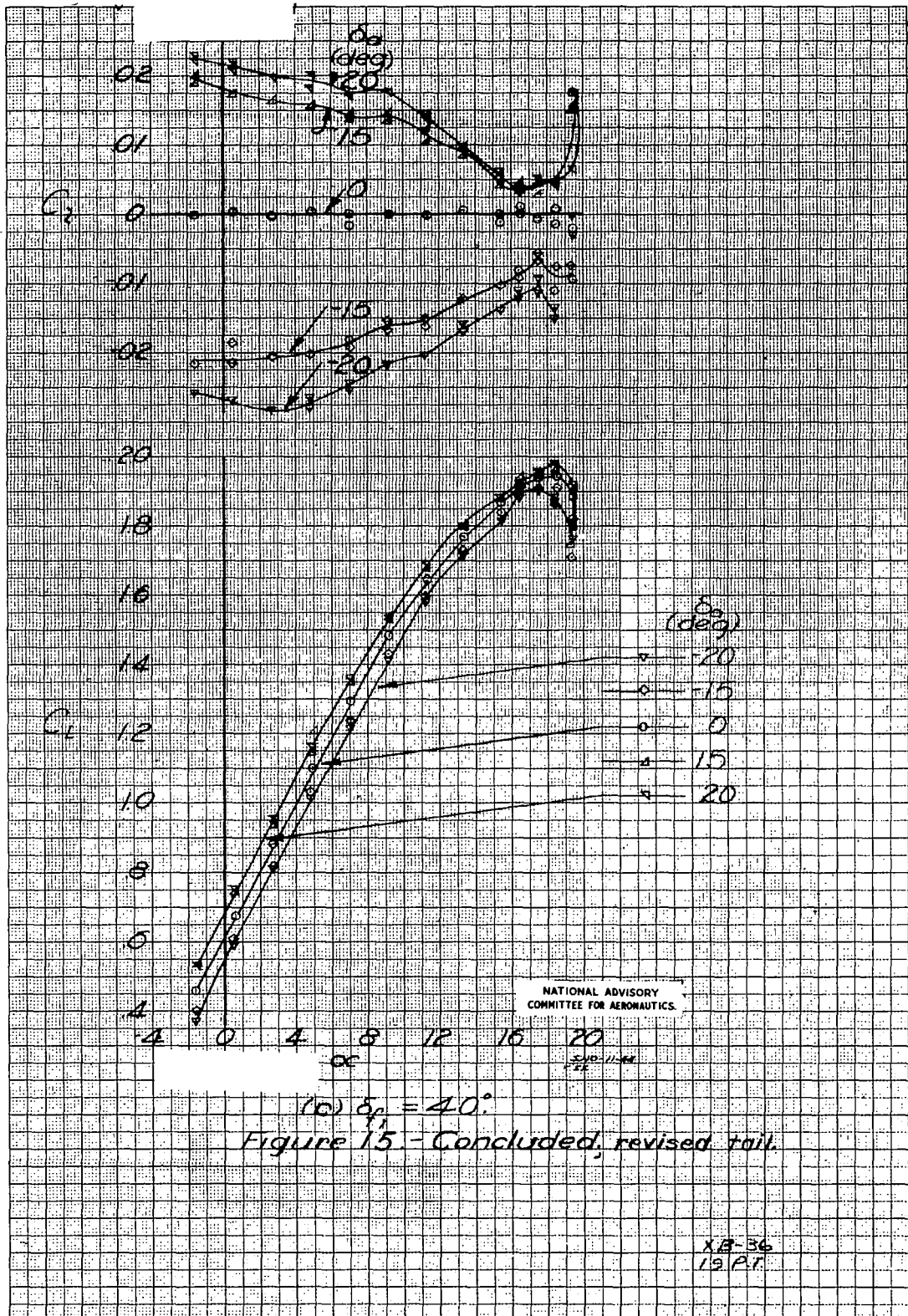


NATIONAL ADVISORY
COMMITTEE FOR AERONAUTICS

(a) $\delta_r = 0^\circ$; $\delta_f = 0^\circ$

Figure 13.- Aileron characteristics of a 1/14-scale model of the XB-30 airplane. Wing W₁; original tail; $Re = 4,500,000$; $M = 0.17$





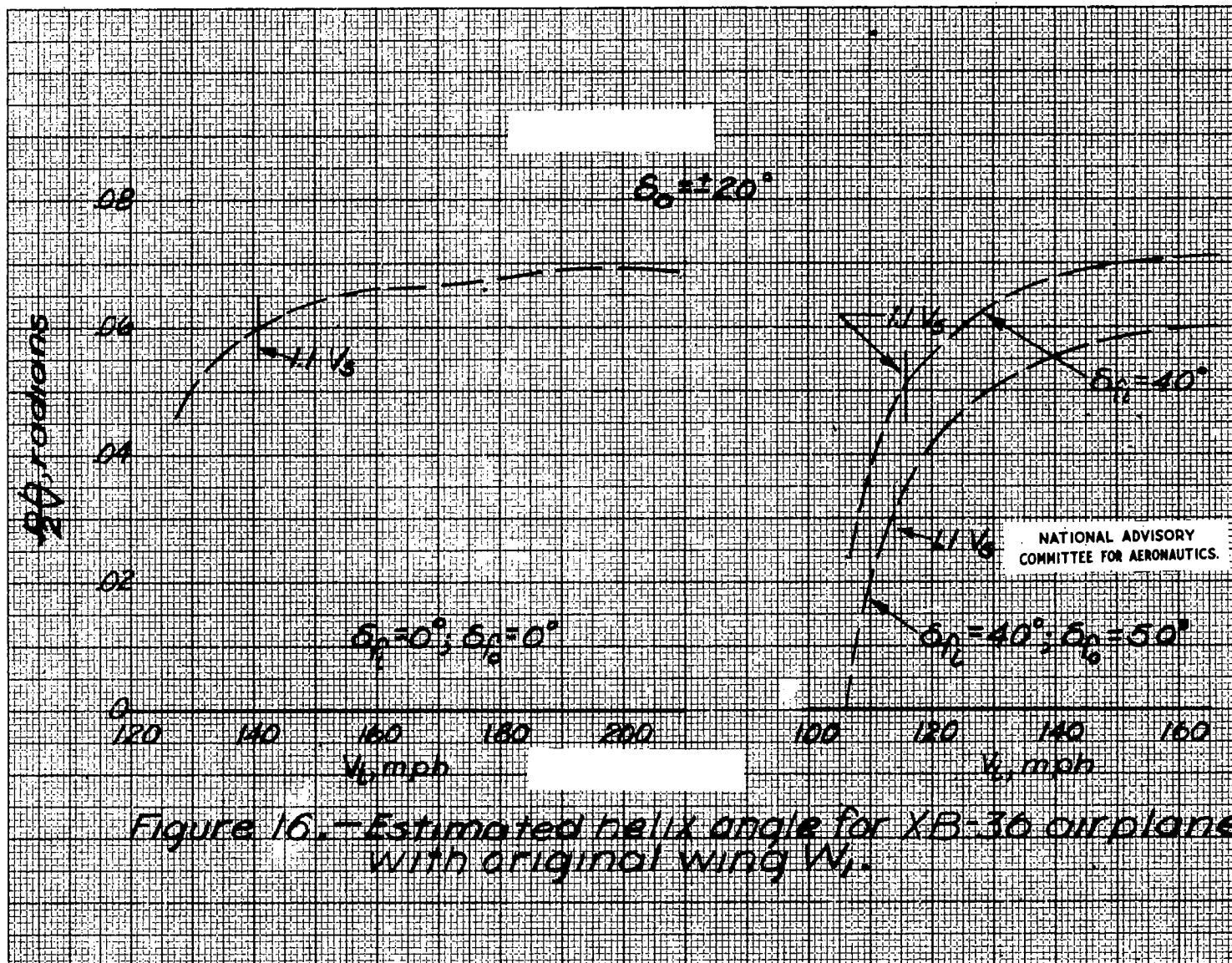


Figure 16. - Estimated helix angle for XB-36 airplane with original wing N_1 .

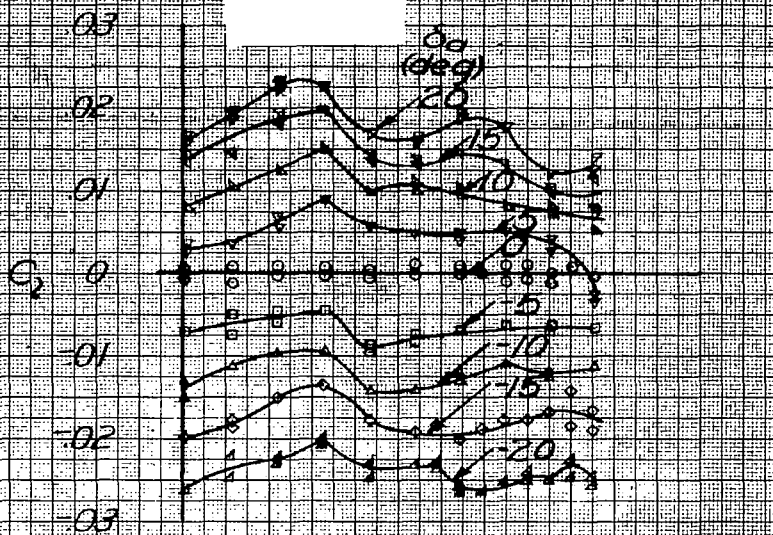
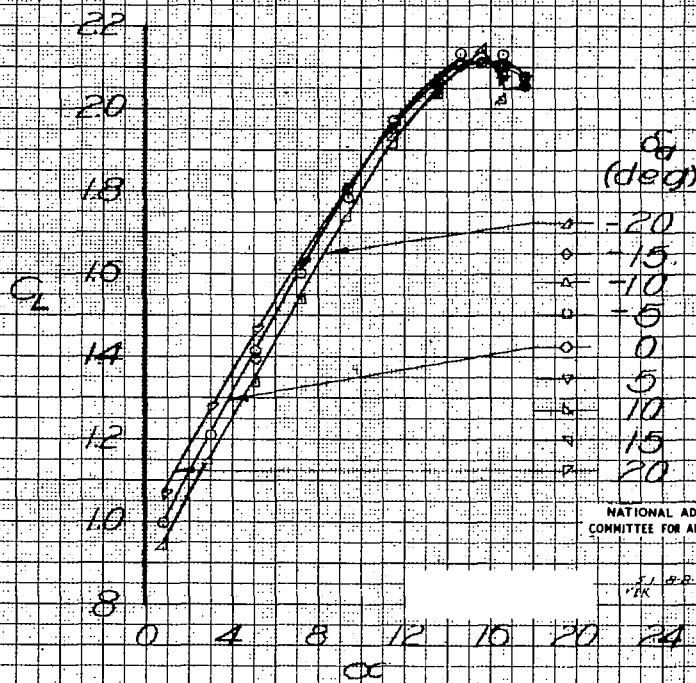
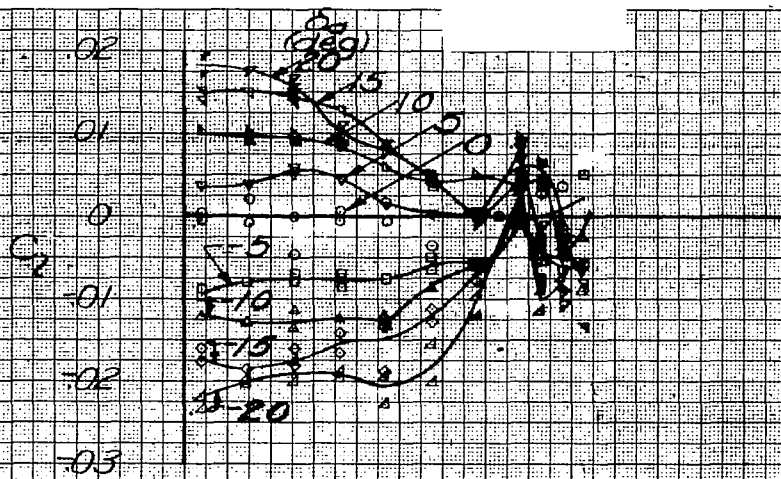


Figure 17 - Aileron characteristics of a 1/14-scale model of the XB-30 airplane. Wing W_2 , $R=4,500,000$, $M=0.17$.



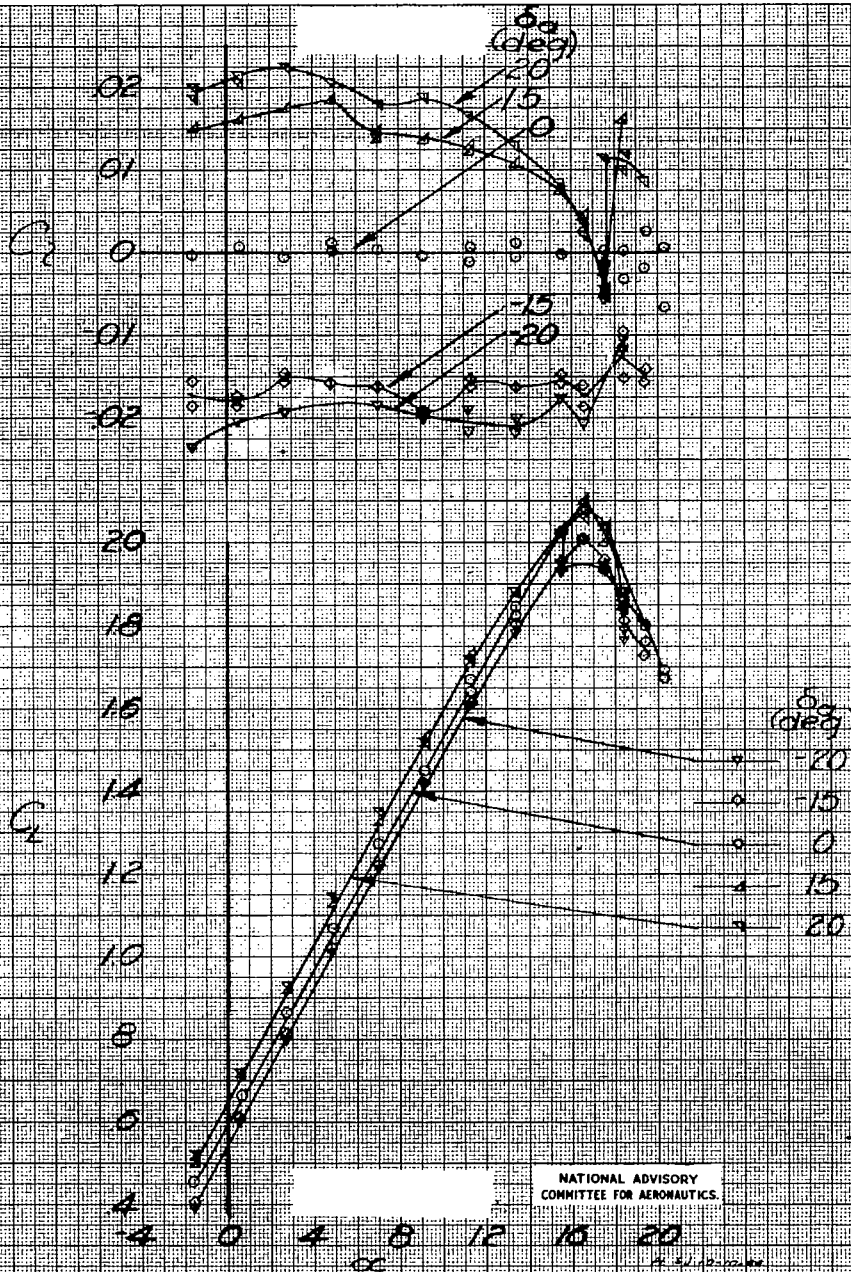
NATIONAL ADVISORY
COMMITTEE FOR AERONAUTICS

11-10-44
11K

(b) $\delta_{f_i} = 40^\circ$; $\delta_{f_o} = 50^\circ$.

Figure 17.-Continued.

XB-30
19 PT

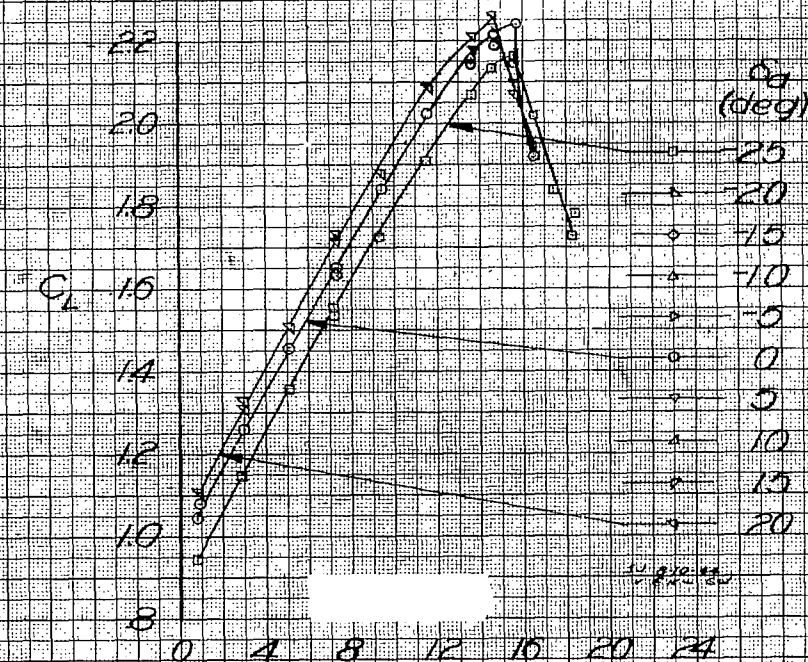
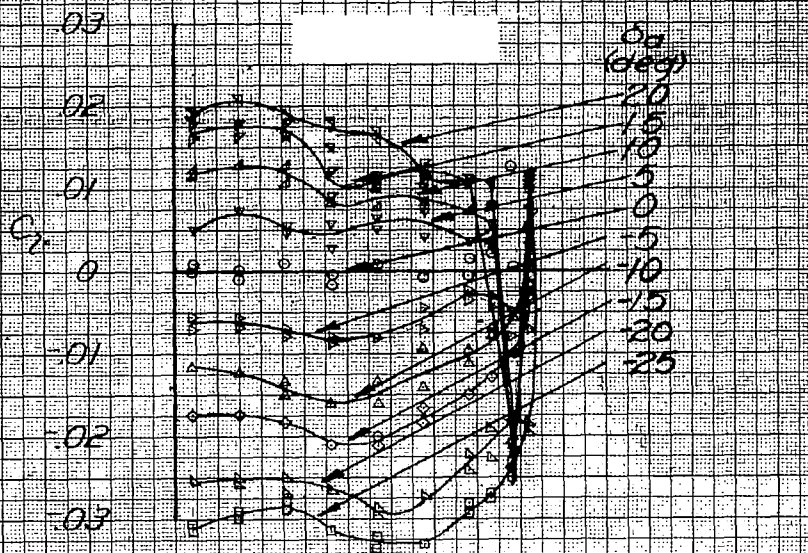


NATIONAL ADVISORY
COMMITTEE FOR AERONAUTICS.

(c) $\delta_z = 40^\circ$

Figure 17 - Continued.

18-36
19 PT

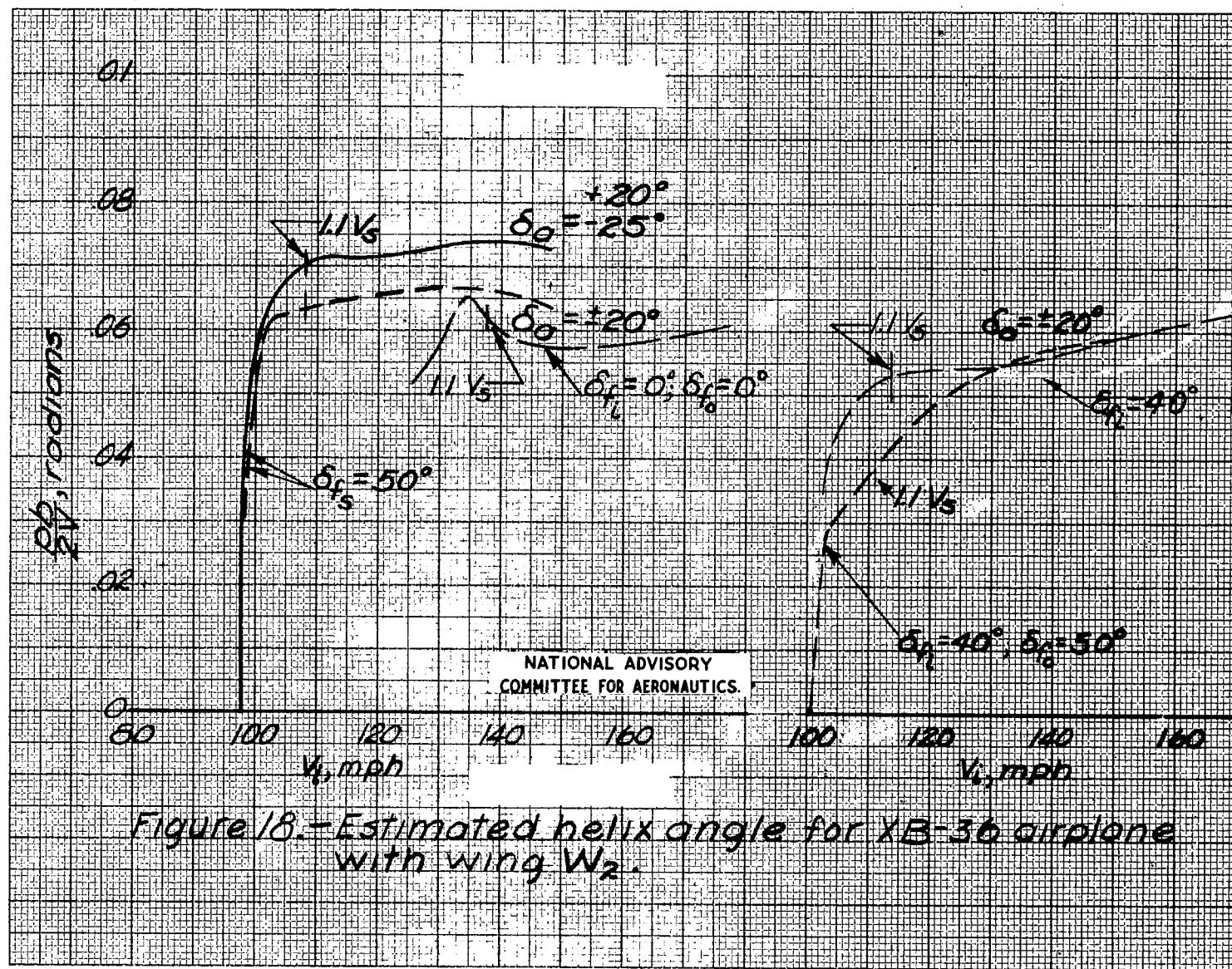


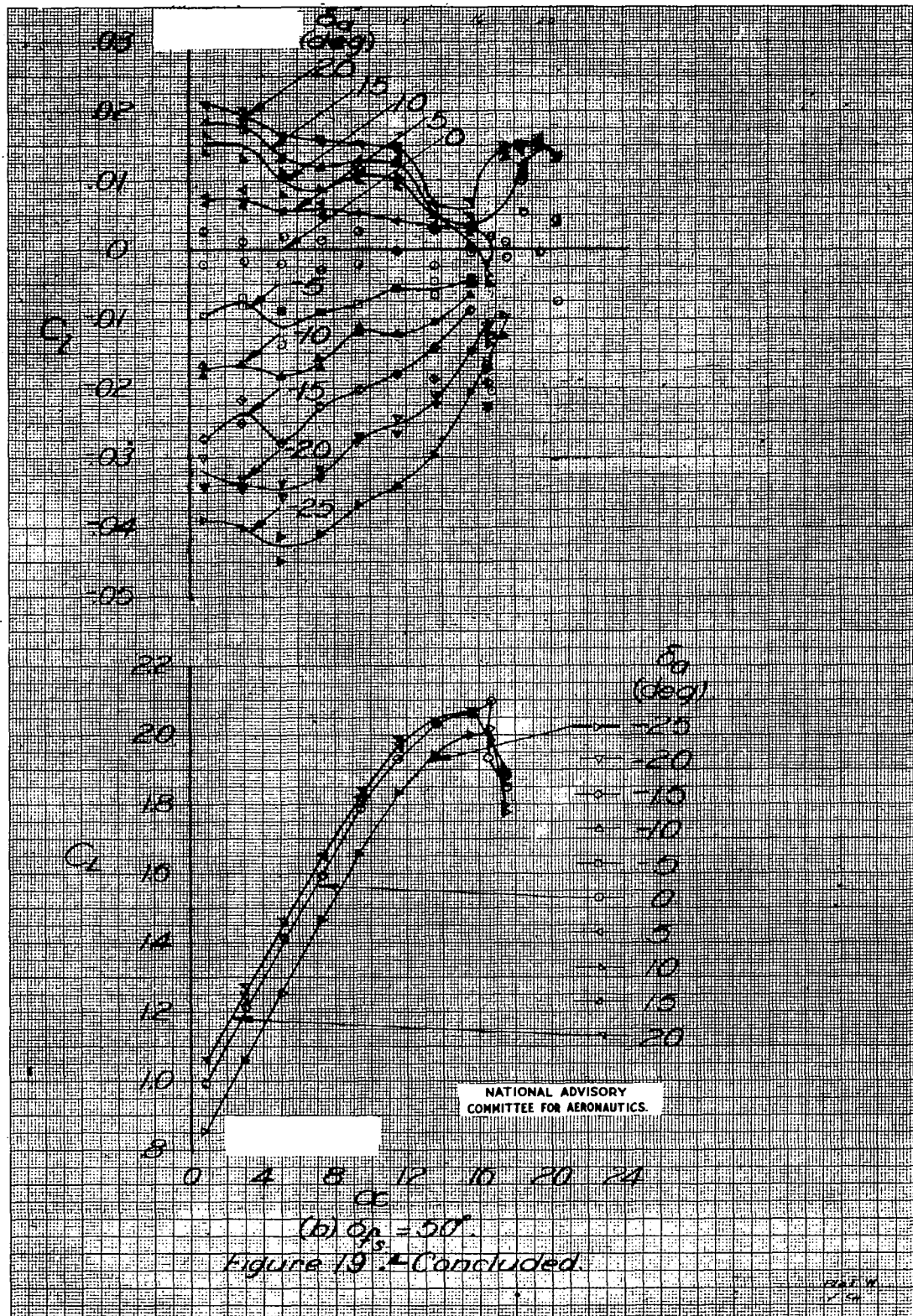
(d) $\alpha_{fs} = 50^\circ$

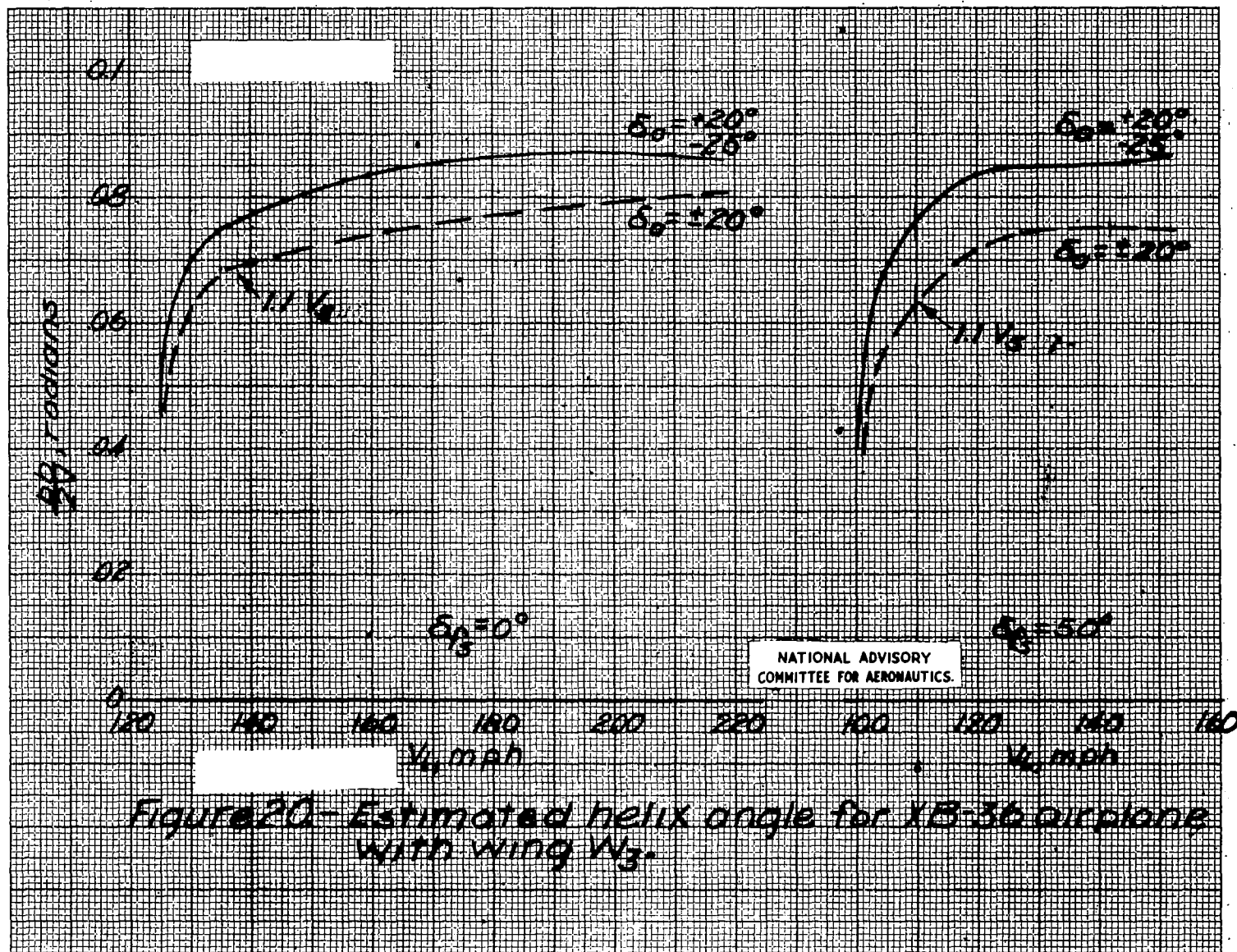
NATIONAL ADVISORY
COMMITTEE FOR AERONAUTICS

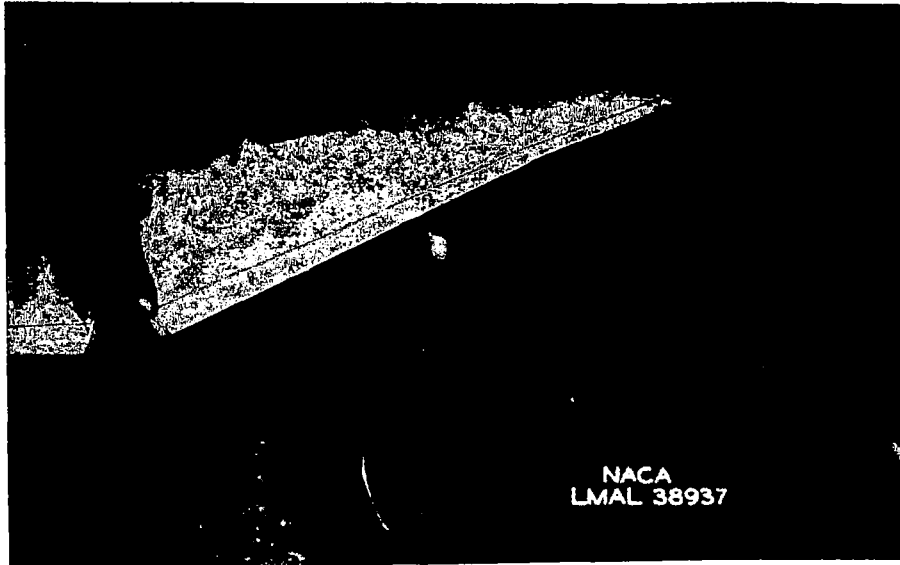
Figure 17.-Concluded

XB-36
19 PT

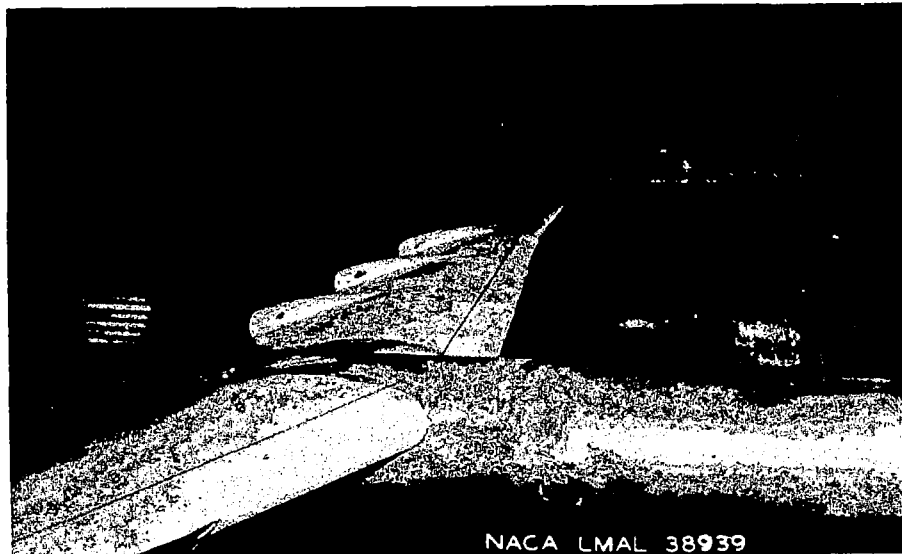








(a) Top view.



(b) Side view.

Figure 21.- Transition strip; $\frac{1}{14}$ -scale model of the XB-36 airplane.

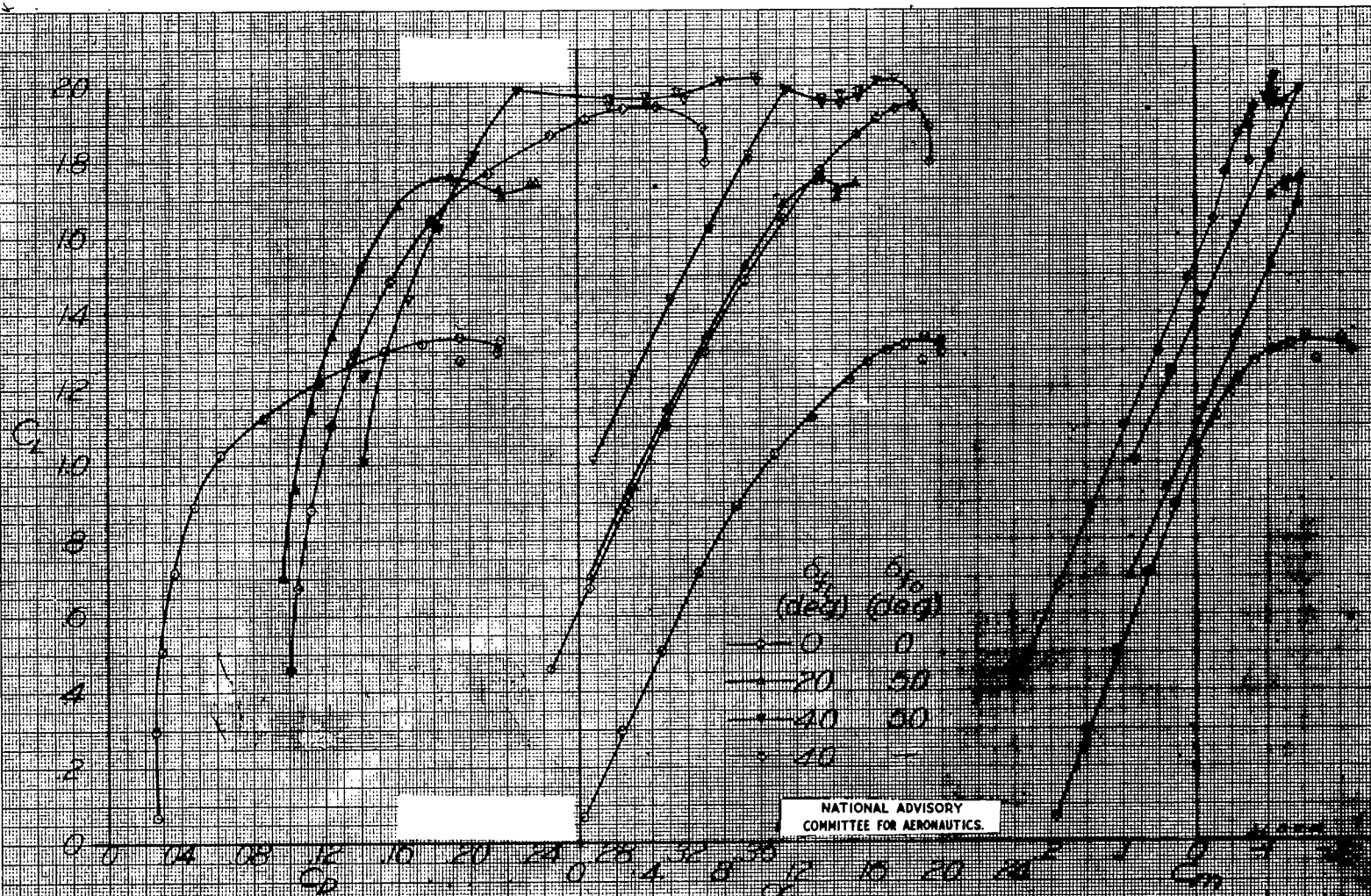
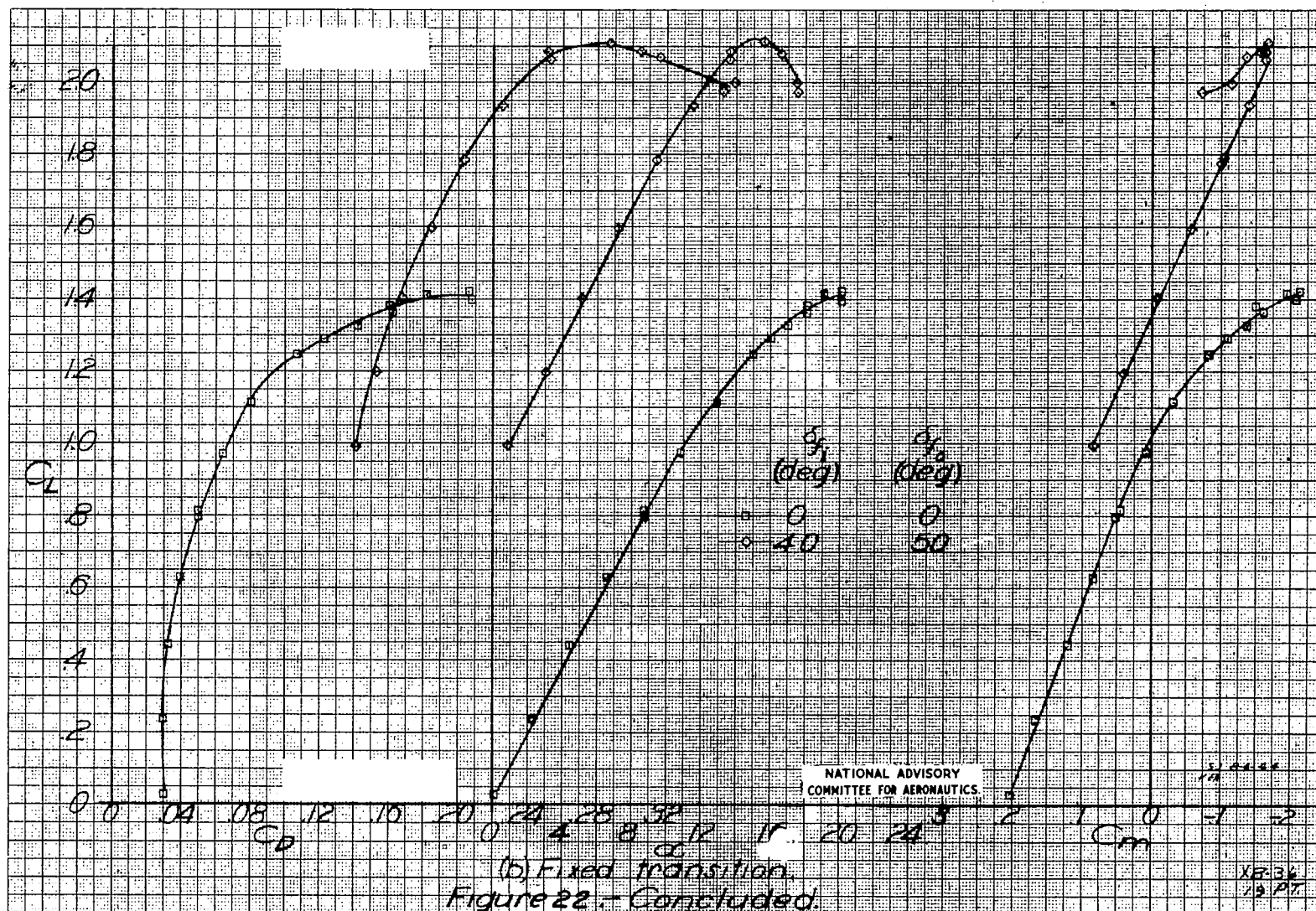
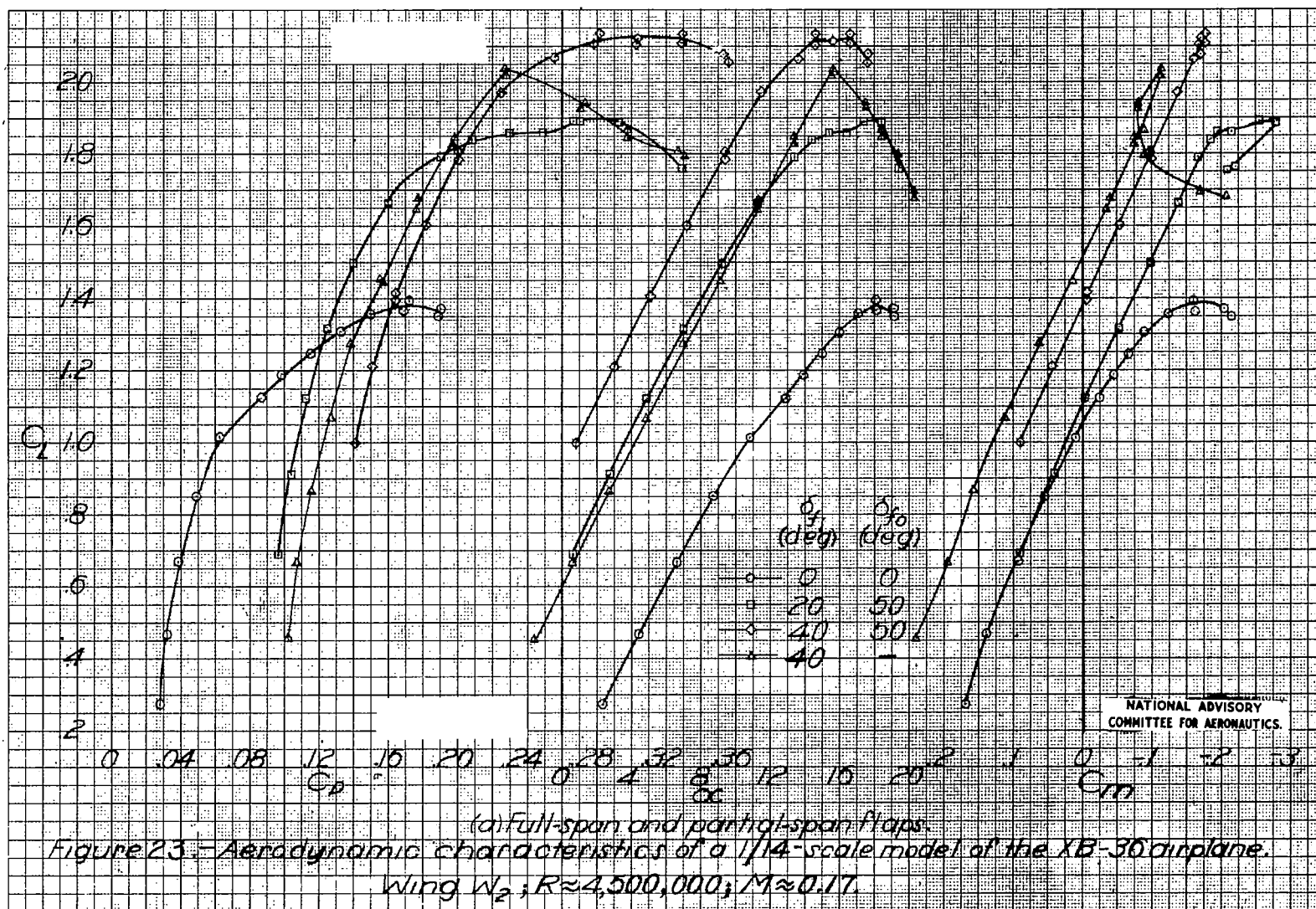
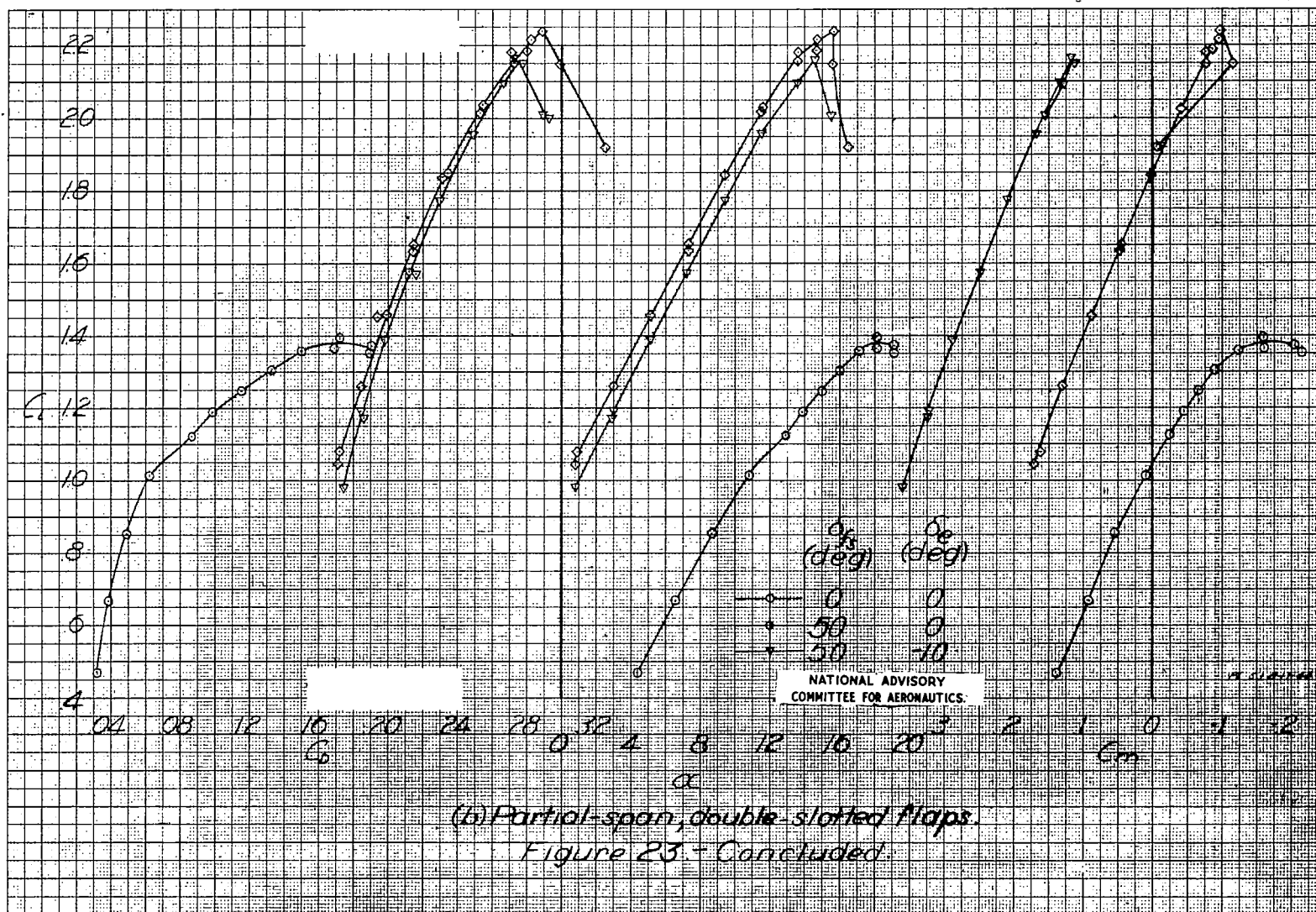
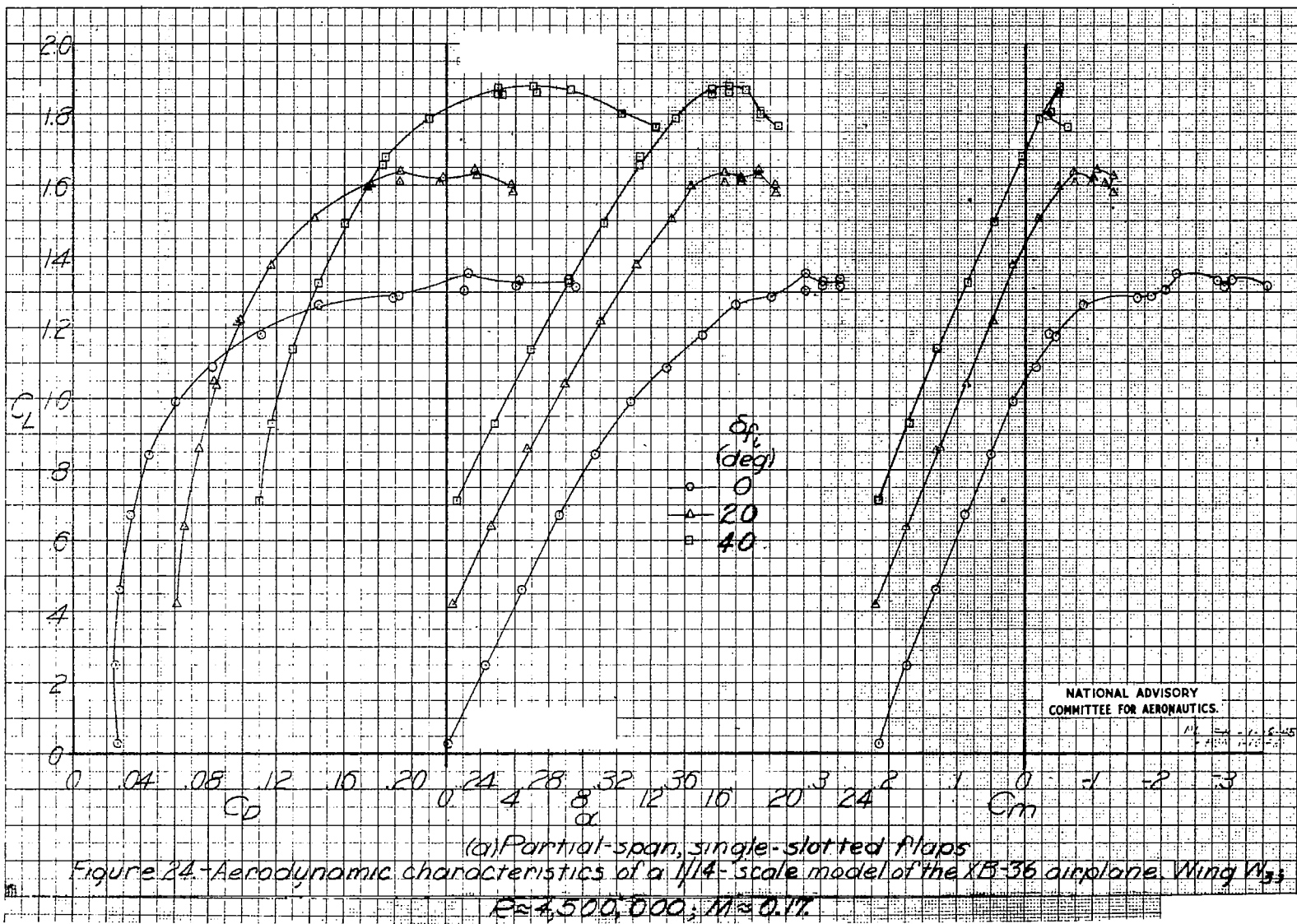


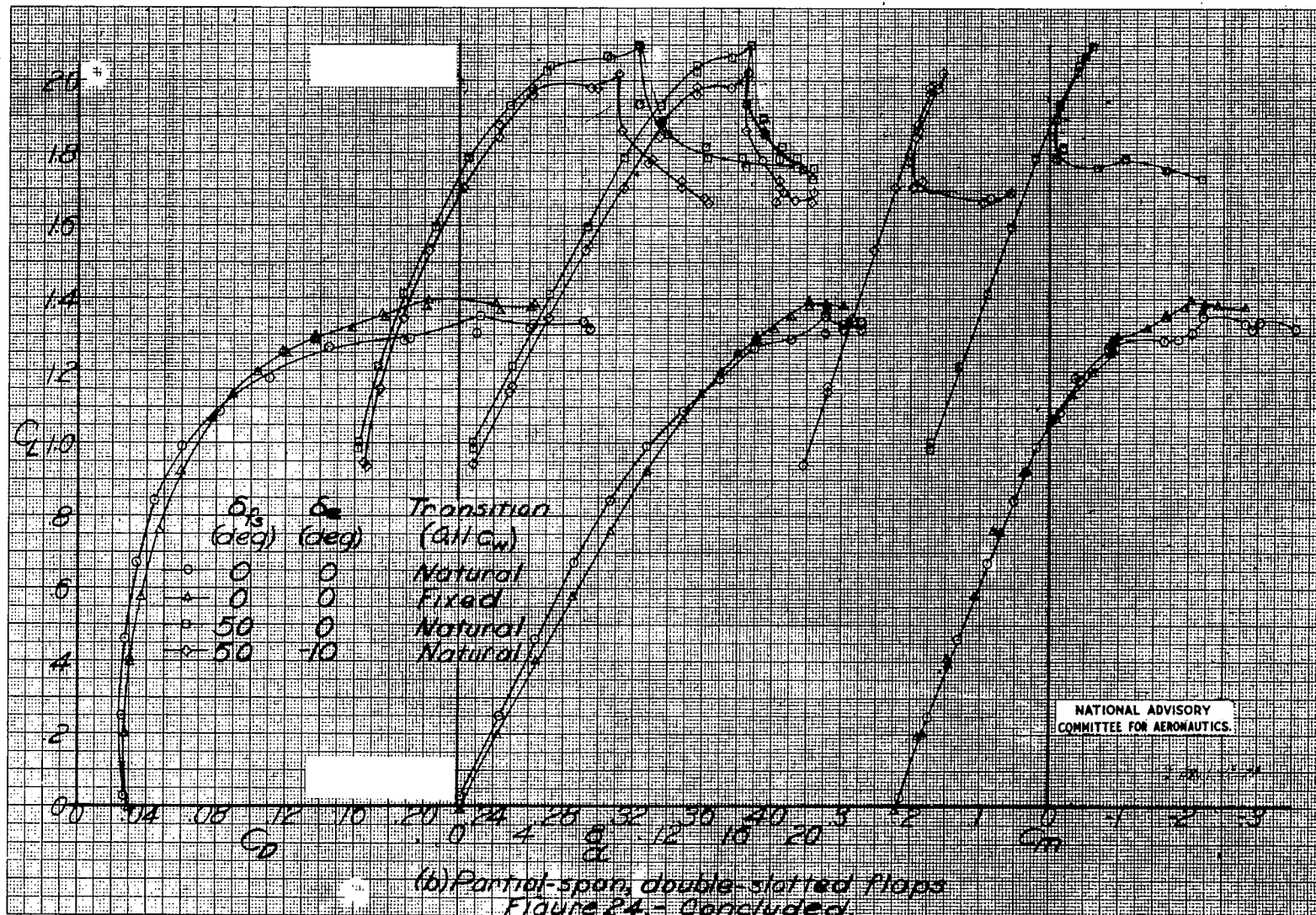
Figure 22. Aerodynamic characteristics of a 1/4 scale model of the X-36 airplane, Ning W.
 $R=1,500,000$; $M=0.17$

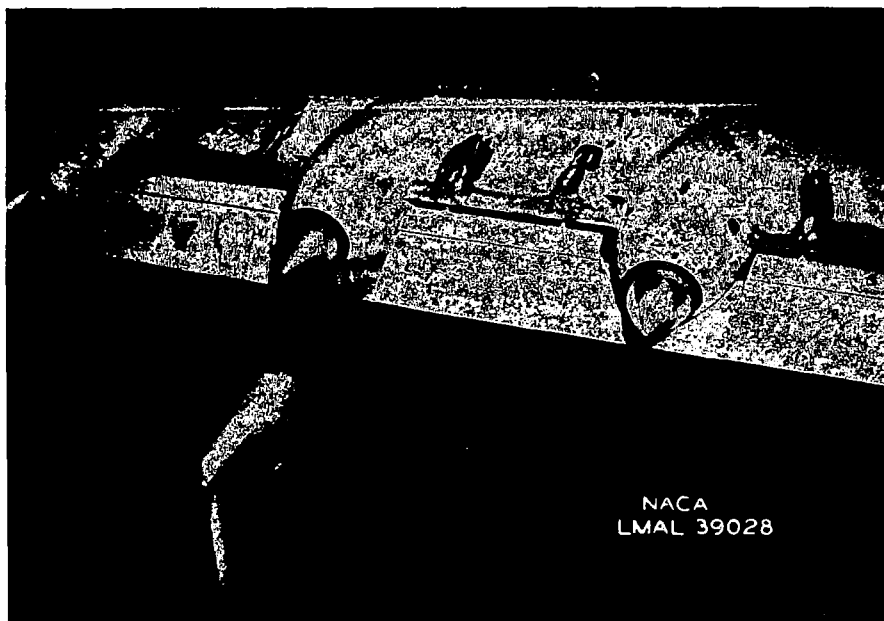




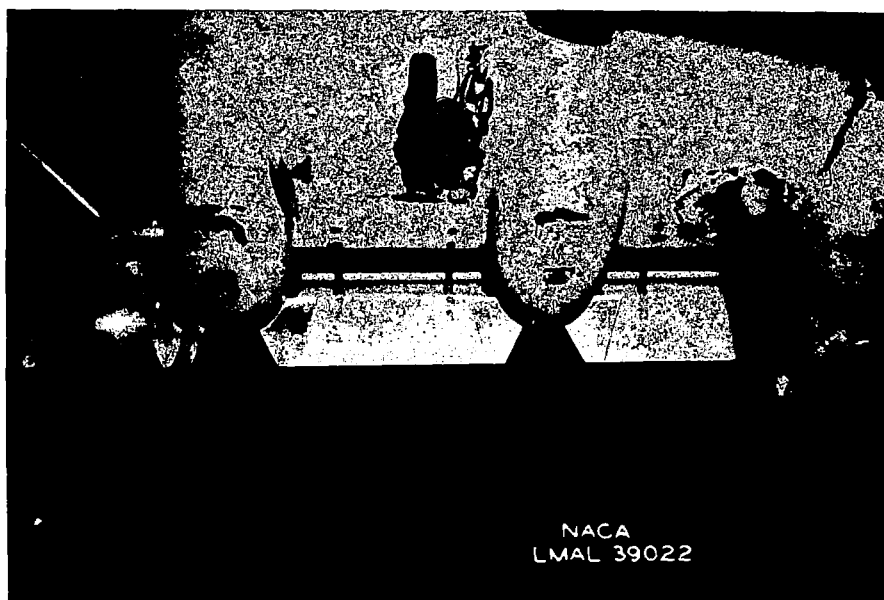








(a) Full seal.



(b) Modified seal.

Figure 25.- Flap-nacelle seals; $\frac{1}{14}$ -scale model of the XB-36 airplane.

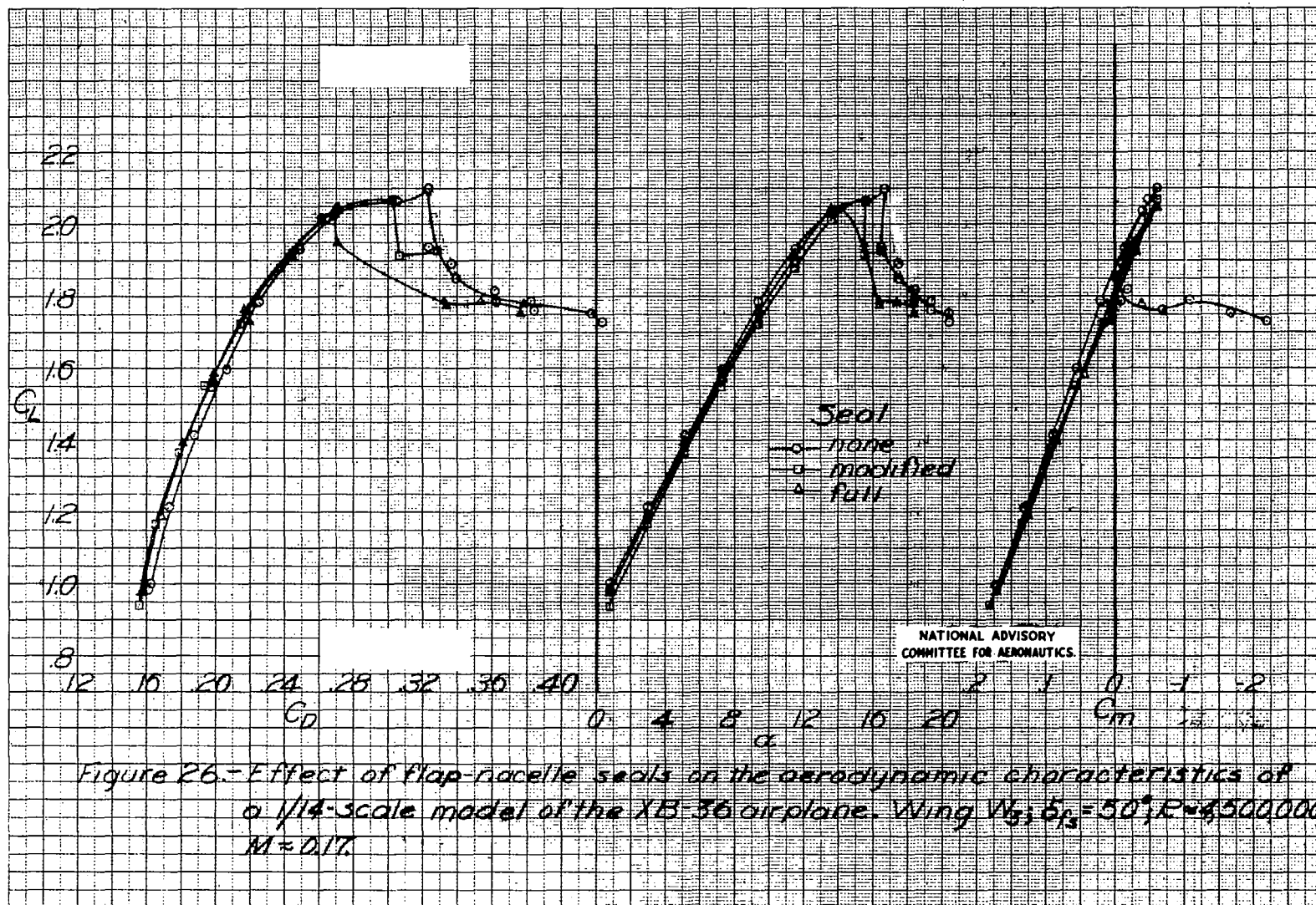


Figure 26.- Effect of flap-nacelle seals on the aerodynamic characteristics of a 1/14-scale model of the XB-36 airplane. Wing V_b ; $S_{ps} = 50$; $R = 4,500,000$; $M = 0.17$.

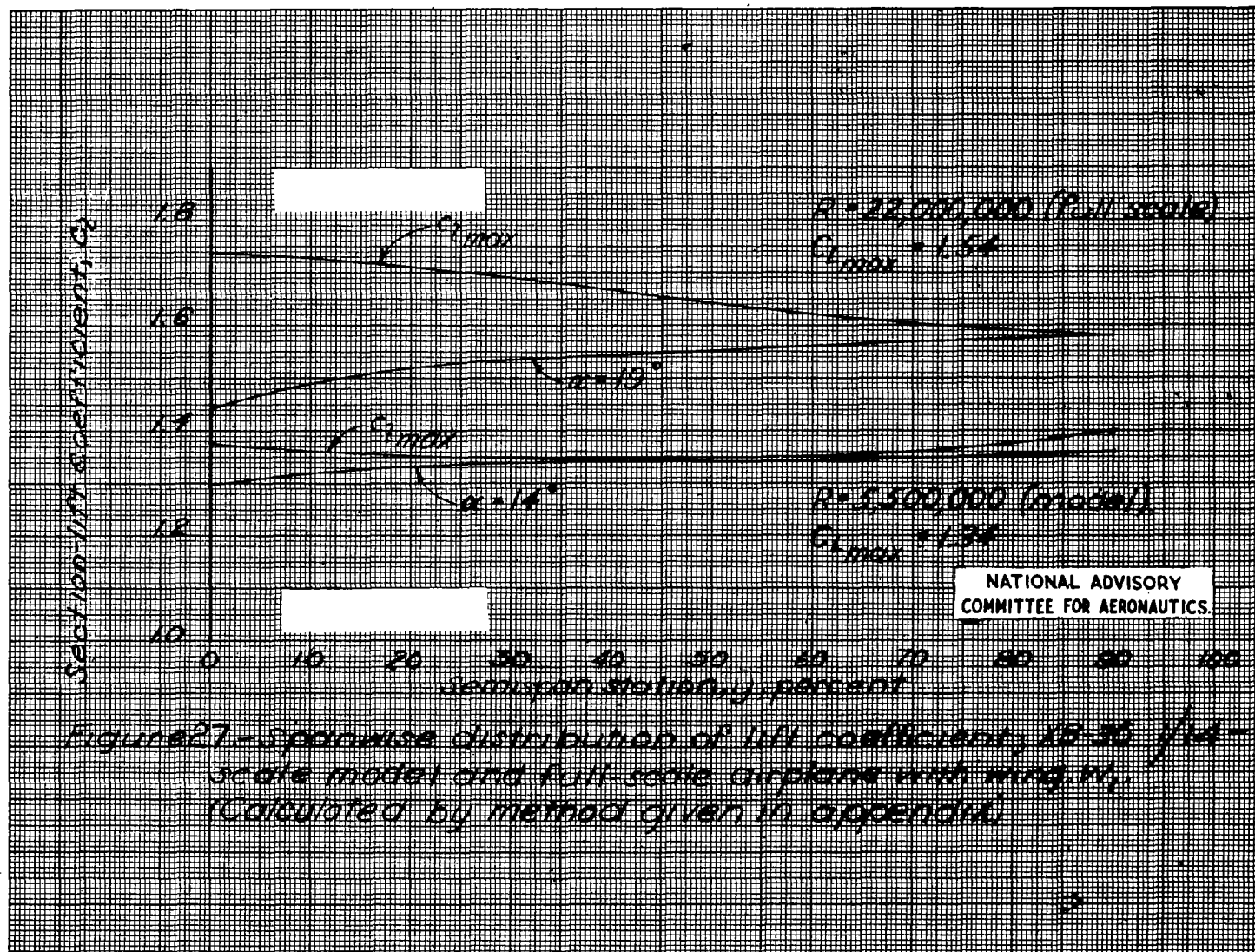
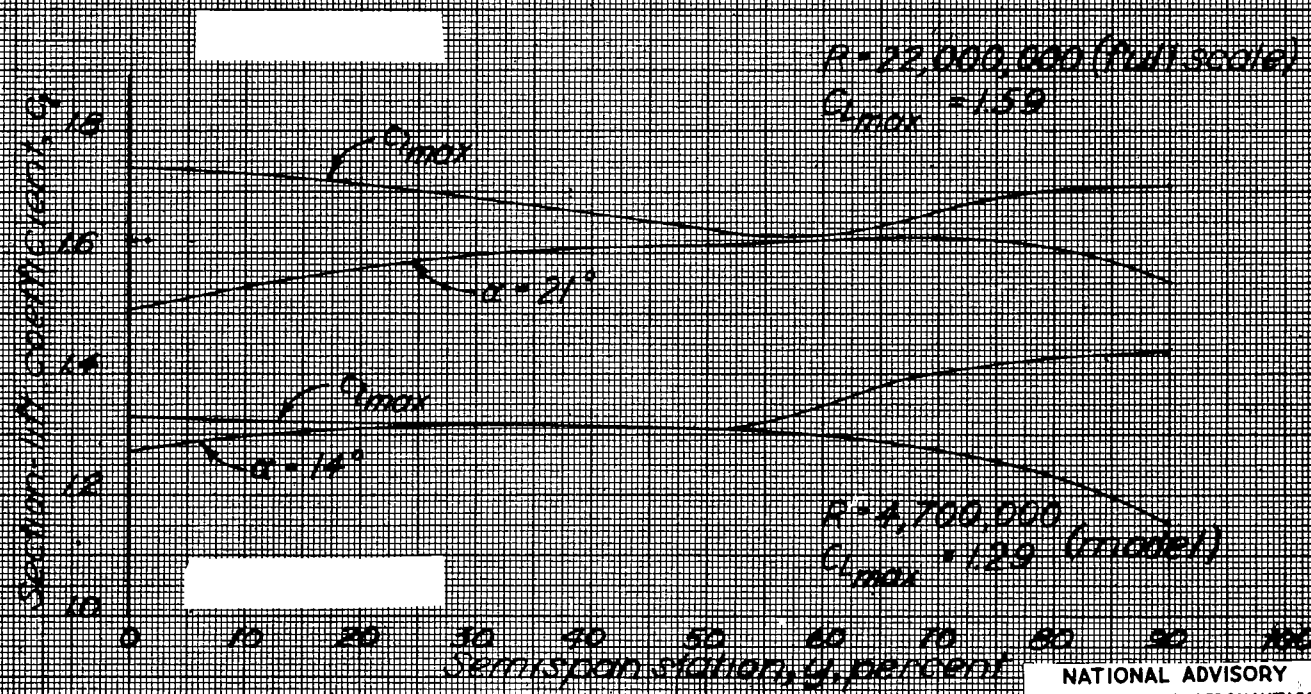


Figure 27. Spanwise distribution of lift coefficient, XB-35 full-scale model and full-scale airplane with wing tip. (Calculated by method given in appendix.)



NATIONAL ADVISORY
COMMITTEE FOR AERONAUTICS.

Figure 28.- Spanwise distribution of lift coefficient, XH-30 1/14 scale model and full-scale airplane with wing W_3 . (Calculated by method given in appendix)

LANGLEY RESEARCH CENTER



3 1176 01354 3815